NASA TECHNICAL REPORT

NASA TR R-258

NASA TR R-258

TRAJECTORY OPTIMIZATION FOR AN APOLLO-TYPE VEHICLE UNDER ENTRY CONDITIONS ENCOUNTERED DURING LUNAR RETURN

by John W. Young and Robert E. Smith, Jr.

Langley Research Center
Langley Station, Hampton, Va.

NATIONAL AERONAUTICS AND SPACE ADMINISTRATION • WASHINGTON, D. C. • MAY 1967

NASA TR R-258

TRAJECTORY OPTIMIZATION FOR AN APOLLO-TYPE VEHICLE UNDER ENTRY CONDITIONS ENCOUNTERED DURING LUNAR RETURN

By John W. Young and Robert E. Smith, Jr.

Langley Research Center
Langley Station, Hampton, Va.

NATIONAL AERONAUTICS AND SPACE ADMINISTRATION

For sale by the Clearinghouse for Federal Scientific and Technical Information
Springfield, Virginia 22151 – CFSTI price $3.00

TRAJECTORY OPTIMIZATION FOR AN APOLLO-TYPE VEHICLE UNDER ENTRY CONDITIONS ENCOUNTERED DURING LUNAR RETURN

By John W. Young and Robert E. Smith, Jr.
Langley Research Center

SUMMARY

This report describes a numerical optimization study conducted to investigate optimal performance boundaries, from considerations of maneuver capability and entry heating, for an Apollo-type vehicle under entry conditions encountered during lunar return. Results presented show the effects on these performance boundaries of variations in initial entry conditions and vehicle characteristics and of constraints on such trajectory variables as altitude and acceleration. The effect of the earth's rotation on optimal performance is also included. Typical trajectories are presented to illustrate and contrast the basic nature of various optimal entry missions.

The results of the study show that there are numerous trade-offs possible between maximum maneuver capability and optimal entry heating. The determining factors for these trade-offs are the initial entry conditions, the trajectory constraints, and the physical characteristics of the entry vehicle. The results also show that, although radiative effects can account for a significant portion of total entry heating, the trajectories for optimal heat entries are largely determined by convective inputs.

INTRODUCTION

It is important for practical reasons and of interest academically to investigate optimal entry trajectories during return from a lunar mission. From a practical standpoint, optimal trajectory data can be used to establish performance boundaries for typical entry vehicles and missions. These boundaries can serve as guides in vehicle and mission design studies and as standards for comparing the operation of various entry guidance schemes.

A number of trajectory optimization studies have been carried out in the past. Two such studies, given in references 1 and 2, present typical trajectories for which entry heating is minimized and for which lateral displacement is maximized. Since these studies, which were of a pioneering nature, were primarily directed toward developing

and illustrating new theories for optimization, only a limited number of trajectory results were presented. The present analysis seeks to expand these previous results into a parametric type of study which includes a number of entry conditions, trajectory constraints, and vehicle characteristics. The objective of the study is to investigate optimal performance boundaries, from considerations of maneuver capability and entry heating, for an Apollo-type vehicle under entry conditions encountered during lunar return. The present analysis makes use of an iterative numerical optimization procedure, based on the method of steepest ascent, to obtain the desired results.

Optimal performance boundaries from a standpoint of maneuver capability and heating are presented for an assumed nominal entry mission. This nominal mission consisted of a parabolic entry into a nonrotating earth's atmosphere by an Apollo-type vehicle with an offset center of gravity which produced a lift-drag ratio of 0.5. Results are presented showing the effect on these performance boundaries of variations in initial entry conditions and vehicle characteristics and of constraints on such trajectory variables as altitude and acceleration. Also included is the effect of the earth's rotation on optimal performance for a number of initial orbital headings. In addition to these summary-type results, typical trajectories are presented to illustrate and contrast the basic nature of the different types of optimal entry missions considered in the analysis.

SYMBOLS

C_D	drag coefficient
g	acceleration due to gravity, meters/second^2 (ft/sec^2)
h	altitude, kilometer (ft)
L/D	lift-drag ratio
m	mass of vehicle, kilograms (lbm)
P_a	acceleration dose (fig. 6)
Q	heat absorbed per unit area at stagnation point, joules/meter^2 (Btu/ft^2)
S	surface area, meter^2 (ft^2)
t	time, seconds

V	velocity, kilometers/second (ft/sec)
γ	flight-path angle, degrees
ρ	density, kilograms/meter^3 (lbm/ft^3)
τ_a	endurance limit to acceleration (fig. 5), seconds
Ω_E	angular velocity of earth, radians/second

Subscripts:

c	convective heat input
i	inertial
o	initial value
r	equilibrium radiative heat input
s	apogee altitude during skip trajectory
x	exit condition for skip trajectory

A dot over a symbol denotes a derivative with respect to time.

ANALYSIS

Computer Program and Optimization Procedures

The results presented in this study were obtained with a three-degree-of-freedom trajectory optimization computer program. A complete description of this program can be found in reference 3. However, for convenience, a brief description of the program is given in the present analysis along with a discussion of the procedures and terminology used.

Computer program capabilities.- The basic function of the computer program is to determine optimal trajectories for point-mass aerospace vehicles. An iterative steepest ascent computational procedure is used to determine control-variable time histories (angle of attack and roll angle) which yield trajectories satisfying specified initial, in-flight, and terminal constraints while optimizing selected functions of the terminal state.

The program has a capability for optimizing individually a wide variety of state variables and functions of state variables. This group of functions, as well as the total stagnation-point heat input and the total acceleration dose, can be specified as terminal inequality or equality constraints. In addition, upper bounds on altitude, heating rate, and acceleration can be included as in-flight constraints.

The computer program treats the vehicle as a mass particle that can accomplish coordinated-turn maneuvers. The earth can be approximated as an oblate spheroid and a rotating earth and atmosphere can be included.

Optimization techniques.- The method used in the present study to obtain performance boundaries for an entry vehicle was to place individually or collectively in-flight and terminal constraints on a trajectory and then to optimize some quantity subject to these constraints. For example, a point on a vehicle's maximum range contour or "footprint" could be obtained by specifying the down range and maximizing the cross range. The condition on down range is a terminal constraint and can be of the equality (one specific value) or inequality (between upper and lower bounds) type.

An additional form of constraint other than the terminal type was an in-flight constraint which was active throughout a trajectory. If, as in the previous example, maximum cross range for a specified down range were desired, with the additional requirement that the altitude should not exceed some upper bound, this altitude limit would constitute an in-flight constraint.

Numerous other terminal and in-flight constraints can be combined to compute a variety of optimal trajectories which are of practical importance in determining performance boundaries for an entry vehicle.

Scope of Study

Performance boundaries were computed for a "nominal" Apollo-type vehicle entering the atmosphere of a spherical earth at near parabolic velocity. The vehicle generally considered in the study was one with a lift-drag ratio of 0.5 and a ballistic parameter m/C_DS of 322 kg/m^2 (2.05 $slug/ft^2$). Lift modulation was achieved by rolling the vehicle which was trimmed to a constant lift coefficient by offsetting the center of gravity.

The nominal initial conditions considered were for entry into a nonrotating atmosphere at an altitude of 121.92 km (400 000 ft) with a velocity of 10.972 km/sec (36 000 ft/sec) and a flight-path angle of -6.5°. These initial conditions are near the center of the available entry corridor during return from a lunar mission. All entries were terminated at an altitude of 30.48 km (100 000 ft) since below this altitude the vehicle is approaching terminal velocity and little control of the trajectory is possible.

Deviations from the previously stated nominal conditions were also studied. The effect on performance of variations in the initial entry angle and velocity of up to $\pm 1^{o}$ and ±1.22 km/sec, respectively, were included. Also considered was the effect of changes in vehicle characteristics. These changes consisted of variations in L/D over the range from 0.2 to 0.5 and changes in the ballistic parameter of up to ±40 percent from the nominal value of 322 kg/m^2. In addition, the effect on performance of entry into an atmosphere which rotated with the earth was studied for various initial heading angles.

Heating considerations included a determination of the total stagnation-point heat input due to convection and equilibrium radiation. The following equations were used for these calculations:

Convective:

$$\dot{Q}_c = 20\rho^{1/2}\left(\frac{V}{1000}\right)^3 \text{Btu/ft}^2\text{-sec} \tag{1a}$$

Radiative:

$$\dot{Q}_r = 6.1\rho^{3/2}\left(\frac{V}{10\ 000}\right)^{20} \text{Btu/ft}^2\text{-sec} \tag{1b}$$

where velocity is in ft/sec and density is in $slugs/ft^3$. An effective nose radius of 1 foot was assumed for both radiative and convective inputs.

Equations (1) are based on an empirical fit to experimental data. The convective heat equation is of a generally accepted form and has been used in numerous studies in the past. The radiative equation is based on results given in reference 4. The coefficients and exponents used in this equation apply only for velocities between about 8.5 and 11.5 km/sec. However, as shown in reference 4, no significant contribution to entry heating due to radiation would occur for velocities below about 8.5 km/sec.

Most of the results to be presented which relate to entry heating include only convective effects. This condition resulted from a greater confidence in the equation and coefficients used to represent convective heating and was due to an uncertainty in the weighting factor between convective and radiative inputs. Although the assumed representation for radiative heating (eq. 1(b)) may be less accurate than that for convective heating, limited radiative results are, nevertheless, presented to bring out some of the interesting features associated with radiative heating. This emphasis on convective heating is, however, not a serious drawback since, as was shown in reference 4 and as will be shown in the present analysis, convective effects account for a large part (about 90 percent) of the total heat input for entry velocities below about 11 km/sec.

Illustration of Optimization Procedure

An example of an entry trajectory which illustrates as well as verifies the operation of the optimization procedure is presented in figure 1. This figure shows a trajectory for which down range was constrained to 1200 international nautical miles and the entry time was minimized. The initial conditions were an altitude of 121.92 km (400 000 ft), a velocity of 10.972 km/sec (36 000 ft/sec), and an entry angle of -6.5^{o}.

The dashed line in figure 1 shows the nominal trajectory which was used to initiate the optimization procedure. This nominal trajectory is determined by specifying an initial control variable (roll-angle) time history. The selection of this control-variable program, which is based on trajectory constraints and the function to be optimized, is of importance in successfully initiating the optimization procedure as well as in reducing the number of iterations required to obtain an optimum solution. For the trajectory shown in figure 1, a nominal roll angle of 70^{o} was used since for this condition the down-range constraint of 1200 nautical miles is satisfied.

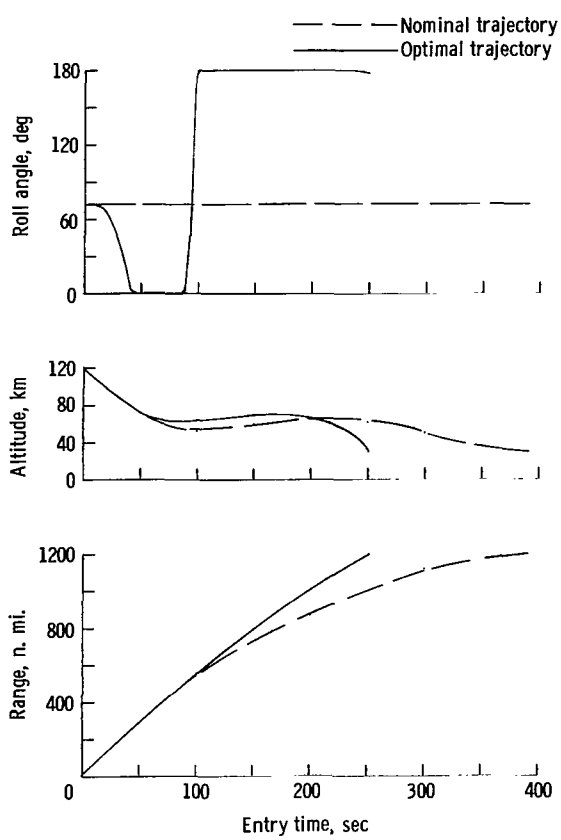

Figure 1.- Nominal and optimal trajectories for minimum time entry. V_0 = 10.972 km/sec; h_0 = 121.92 km; γ_0 = -6.5^{o}; $m/C_D S$ = 322 kg/m^2; L/D = 0.5.

The solid line in figure 1 shows the trajectory obtained after several iterations of the optimization procedure. Modifications in the roll-angle time history have resulted in a 40-percent reduction in the entry time for this trajectory as compared with the nominal trajectory. The shape of the roll-angle curve in figure 1 is of considerable interest. Note that, the initial portion being excluded, the roll-angle variation approaches a condition such that either maximum positive lift (roll angle, 0^{o}) or maximum negative lift (roll angle, 180^{o}) is employed throughout the trajectory. Thus a bang-bang type of control is approached; this result is in agreement with theory for time optimal control systems. (See ref. 5.)

It should be emphasized that the data presented in figure 1 and to be presented throughout the report represent only a near-optimal solution. For example, the data of figure 1 were obtained with 12 iterations of the optimization program. An additional 12 iterations, which doubled the computing time,

led to small changes in the roll-angle history and caused it to approach the ideal bang-bang control more closely, but resulted in no significant reduction in entry time. Thus, to conserve computer time, the results presented in this report were obtained by terminating the convergence procedure after the function to be optimized had approached the true optimal within practical limits.

RESULTS AND DISCUSSION

Maximum Maneuver Capability

The maneuver capability or terminal footprint for an Apollo type vehicle with an offset center of gravity was determined for a variety of initial entry conditions and trajectory constraints. This footprint was determined by maximizing the cross range of the vehicle subject to various in-flight and terminal constraints. The results to be presented in this section were obtained for a vehicle with a lift-drag ratio of 0.5, an m/C_DS of 322 kg/m^2, and an entry altitude of 121.92 km. The effects of changes in lifting capability and ballistic parameter of the vehicle are presented in later sections of the report. Unless specified otherwise, a nonrotating earth and atmosphere are assumed.

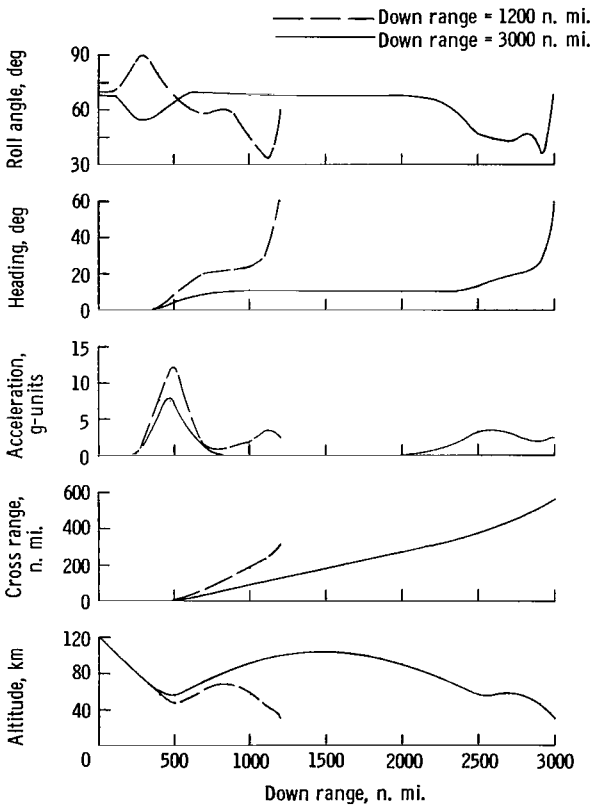

Figure 2.- Typical maximum cross-range entry trajectories. V_0 = 10.972 km/sec; h_0 = 121.92 km; λ_0 = -6.5°; m/C_DS = 322 kg/m^2; L/D = 0.5.

Effect of entry angle on maneuver capability.- Shown in figure 2 are typical maximum cross-range trajectories for entries with down range constrained to 1200 and 3000 nautical miles. These results are for an entry velocity of 10.972 km/sec (36 000 ft/sec) and an initial flight-path angle of -6.5°.

Except for the roll-angle histories, the variations shown in figure 2 are very similar for both the short- and long-range trajectories. For both trajectories maximum cross range is attained by executing a heading change during the initial pullup and then proceeding on a near-constant heading (during which the vehicle is in a near-ballistic path) until the end of the entry is approached at which time an additional heading change is made. For the

short range entry the initial change in heading is greater since less upward lift is required and, hence, more lift can be directed laterally. (It should be recalled that, for the assumed vehicle, maximum upward lift occurs for a roll angle of 0^{o}; maximum downward lift, for a roll angle of 180^{o}; and maximum side force, for a roll angle of $\pm 90^{o}$).

The general effect of entry angle on maneuver capability is given in figure 3. Shown here is a portion of the terminal footprint at entry angles of -5.5^{o}, -6.5^{o}, and -7.5^{o} as well as the convective heating which results during these entries. The trend is as expected, shorter minimum down ranges occurring for the steeper entry angles and greater maximum cross ranges generally occurring for the shallower entry angles. As figure 3 shows, the convective heating increases as down range increases and the heating is smaller for the larger entry angles. For a specified down range, the initial acceleration pulse is greater for the steeper entry angles and results in a reduced total heat input as is shown in a later section of the report.

Included in figure 3 are ranges up to 3600 nautical miles from the entry point. The computing time for longer ranges is prohibitive because of the long flight times resulting from the skip maneuvers required to attain those ranges. Computational difficulties also arise in the convergence procedure for these skip trajectories because of the extreme sensitivity of range to changes in the control-variable program during the initial pullup phase of the entry. Thus, complete entries involving long skip trajectories were not included in the present study. However, some general effects of interest during skip maneuvers are considered in a later section of the report.

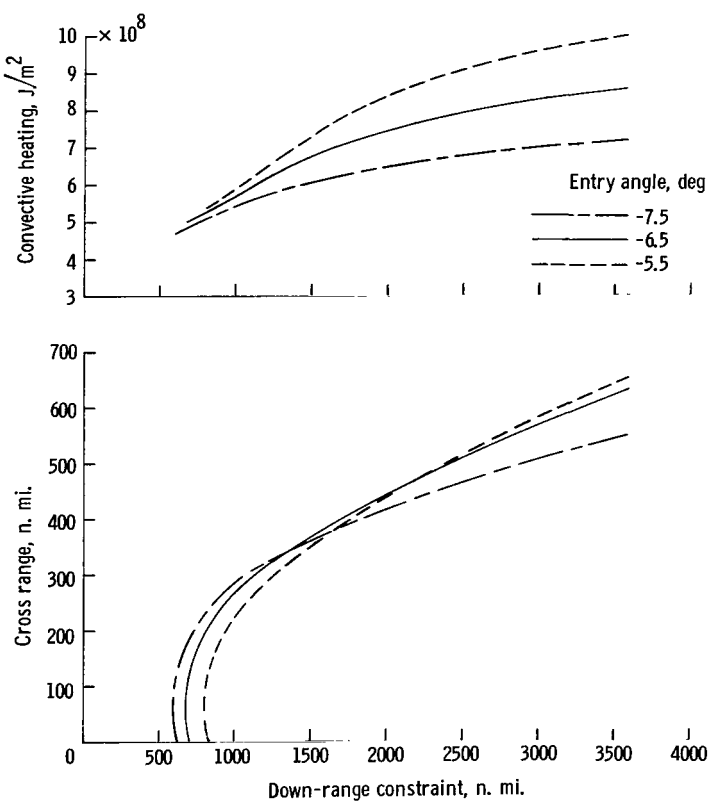

Figure 3.- Effect of entry angle on maximum range capability and resultant convective heating. $V_0 = 10.972$ km/sec; $h_0 = 121.92$ km; $m/C_D S = 322$ kg/m^2; $L/D = 0.5$.

Entries with ranges near the upper and lower limits given in figure 3 are of particular interest. At the upper limit the possibility of limiting the skip altitude exists, whereas at the lower limit the requirement for constraining acceleration arises. An analysis

of these two flight modes is given in the subsequent sections. Unless specified otherwise, the results presented throughout the remainder of this report are for an entry angle of -6.5°.

Effect of altitude constraint on maneuver capability.- Entries with ranges between about 1800 and 3600 nautical miles can be achieved by performing either a direct or skip entry. Certain advantages exist for each type of trajectory. During a skip entry the vehicle spends a portion of the trajectory outside the atmosphere and this condition results in reduced aerodynamic heating. However, from a trajectory-control standpoint, a direct entry might be preferred since aerodynamic forces can be applied to the vehicle throughout an entry. The effect of altitude constraints on the maximum maneuver capability of an entry vehicle is now examined with the aid of figure 4.

Figure 4(a) shows the effect of an altitude constraint on a maximum cross-range trajectory with a down range of 2400 nautical miles. Shown in this figure are trajectories with no altitude constraint and with the skip altitude limited to 80 km (260 000 ft). This limit was chosen since, above this altitude, aerodynamic forces are insufficient for effective trajectory control.

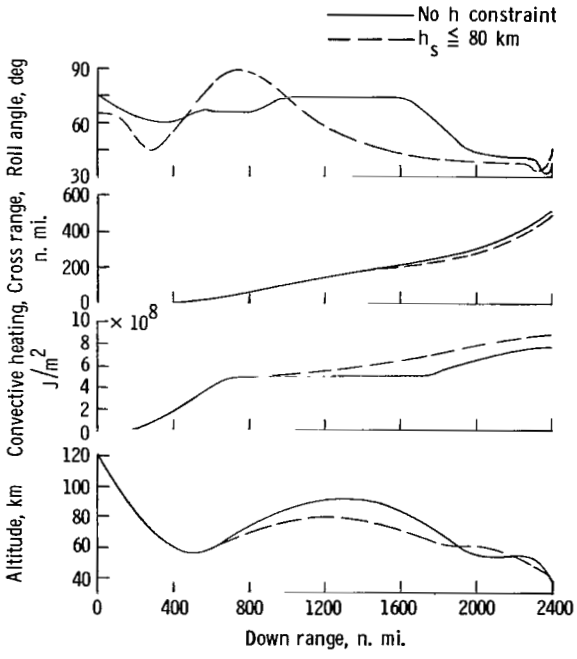

(a) Typical maximum cross-range trajectories with altitude constraint included.

Figure 4.- Effect of altitude constraints on maximum cross range and resultant convective heating. V_0 = 10.972 km/sec; h_0 = 121.92 km; γ_0 = -6.5°; m/C_DS = 322 kg/m^2; L/D = 0.5.

An examination of figure 4(a) shows that for the unconstrained trajectory, the vehicle executes a skip maneuver and follows a near-ballistic path for a part of the entry. During this period no control of the trajectory is possible; thus, the roll angle remains constant at the reference value. For the trajectories presented in figure 4(a) the maximum cross range is nearly the same, only a 3-percent reduction resulting from the altitude constraint. However, because of the reduced altitude profile for the constrained trajectory, an increase of about 15 percent in the convective heating occurs.

As the data of figure 4(a) are for a down-range condition of 2400 nautical miles, it is of interest to examine the effect of an altitude constraint on maneuver capability and heating for other down-range conditions. This effect is shown in figure 4(b) for ranges between 1300 and 3600 nautical miles. As

in figure 4(a), trajectories are given with no altitude constraint as well as with an altitude constraint of 80 km imposed.

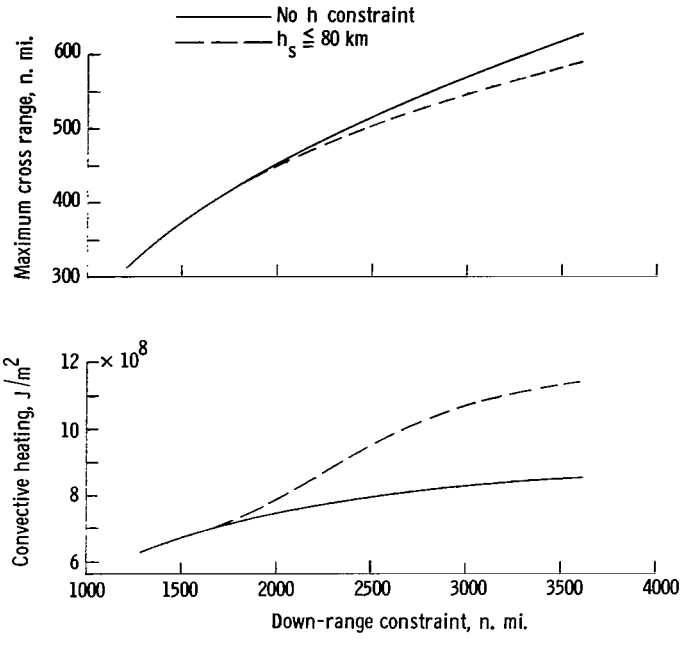

(b) General effect of altitude constraint on maximum cross range and resultant convective heating.

Figure 4.- Continued.

The results of figure 4(b) follow the same pattern as that of figure 4(a), the altitude constraint leading to small reductions in the maneuver capability but causing a considerable increase in convective heating. For example, between the down-range limits of 1800 and 3600 nautical miles, the reduction in cross range varies from 0 to about 6 percent and over the same region the increase in heating varies from 0 to about 35 percent. Although the heating levels given in figure 4(b) for the altitude-limited trajectories may not appear to be excessive, it should be stated that they approach the maximum heating attainable for comparable down-range conditions as is shown in a later section.

The effect on maximum maneuver capability and heating of varying the altitude constraint is given in figure 4(c) for down-range conditions of 1200, 1800, and 2400 nautical miles. The upper altitude limit for each down range (85 km for 1800 nautical miles down range) corresponds to the skip altitude attained for maximum cross-range entries with no altitude constraint imposed (fig. 3). Thus, reduction in the altitude constraint from these peak values must lead to reductions in the maximum cross range as is shown in figure 4(c). (If, for some reason, the maximum skip altitude was specified to be greater than the upper limits of figure 4(c), a reduction in the maximum cross range would again result.) The lowest altitude limits shown in figure 4(c) (62 km for 1800 nautical miles down range) correspond approximately to the minimum altitude constraint which can be imposed and still allow the down-range condition to be satisfied.

In general, figure 4(c) shows that for a particular down range, large decreases in the skip-altitude limit from its unconstrained value lead to small reductions in the maximum cross range. However, as the lower altitude limit is approached, small changes in the altitude constraint result in large reductions in maneuver capability since lift must

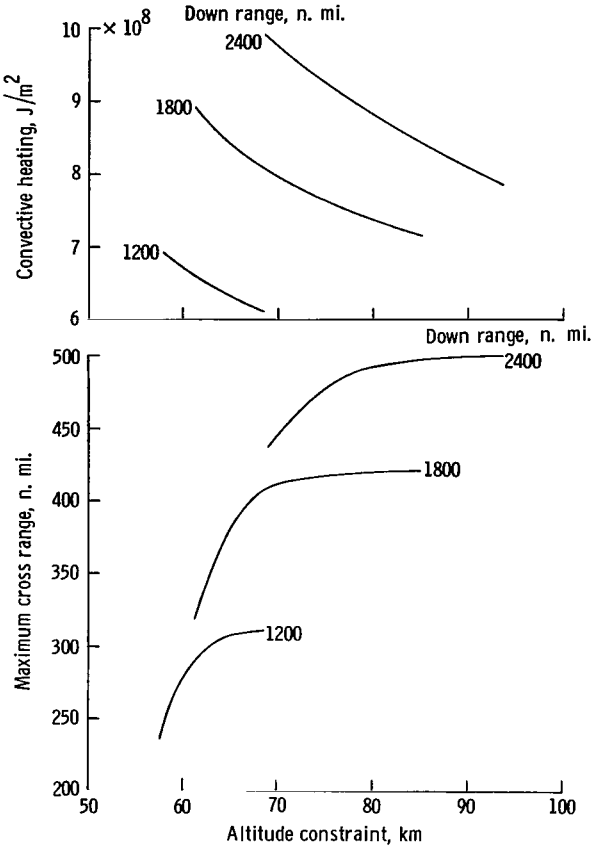

(c) Effect of varying altitude constraint on maximum cross range and resultant convective heating.

Figure 4.- Concluded.

be directed largely into the vertical plane to achieve the required down range. Figure 4(c) also shows that, for the range of conditions shown, convective heating increases almost linearly with decreases in the maximum skip altitude.

Effect of acceleration constraint on maneuver capability.- For ranges less than about 1000 nautical miles, a need exists for limiting the acceleration levels of the assumed vehicle. One approach would be to constrain the peak acceleration during entry. Another approach, which is possibly more realistic for manned entry missions, is to limit the acceleration dose acquired. This approach is used in the present analysis.

The concept of an acceleration dose involves computing a weighted sum of acceleration over the entire trajectory. The weighting factor is based on the acceleration loads which can be endured during entry without impairing a person's ability to perform necessary piloting functions. Several centrifuge studies have been made in the past to determine realistic endurance limits for human pilots. The limits used in the present study were based on the results of reference 6 and are given in figure 5. (The endurance limits shown are for an acceleration directed through the pilot's chest, from front to back.)

Figure 5 shows the endurance limit in seconds as a function of the acceleration level in g units. For a particular acceleration this figure gives the time in which a pilot can function properly. For example, a pilot can sustain an acceleration of 12g for up to 60 seconds and continue to perform his assigned tasks.

The curve shown in figure 5 is incorporated into the optimization procedure in the following manner. Throughout an entry an acceleration penalty function P_a is accumulated by integrating the reciprocal of the endurance limit corresponding to whatever value of acceleration the vehicle is subjected $\left(P_a = \int_0^t \frac{dt}{\tau_a}\right)$. If, at the end of an entry, P_a

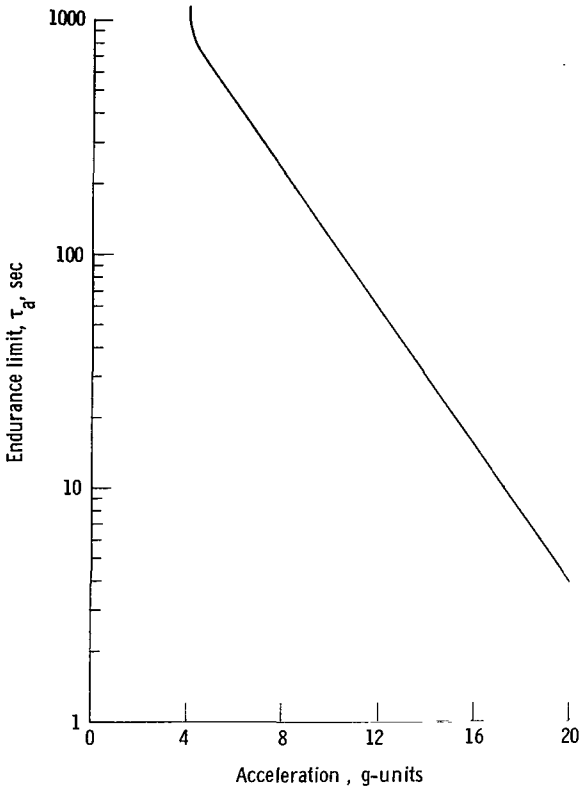

Figure 5.- Acceleration dose curve showing endurance limit to various levels of acceleration.

is greater than unity, an excessive acceleration dose has been acquired, whereas for final values of P_a less than 1.0, the pilot has been subjected to a smaller acceleration load than could have been tolerated. Thus, P_a can be treated as a problem constraint and can be limited to whatever terminal value is desired. It should be noted that, although no extensive experimental justification exists for the use of acceleration dosage as a performance criterion, the concept is mathematically convenient.

Figure 6(a) shows a typical trajectory of the type for which an acceleration constraint is required. Shown in this figure is an entry with nominal entry conditions for which the down range was minimized subject to the condition that the acceleration dose is less than or equal to 1.0. If acceleration were not limited, maximum negative lift would obviously be employed to achieve minimum down range which would result in unreasonable vehicle loads. The roll-angle history of figure 6(a) shows that as the acceleration starts to increase, the roll angle is reduced to increase upward lift and hence to limit the peak acceleration. Thus the range is minimized while acceleration is restrained to acceptable levels.

Since only an acceleration constraint was imposed on the minimum range trajectory of figure 6(a) a final cross range of about 100 nautical miles results for this entry. This lateral offset occurs since, for the assumed fixed-angle-of-attack vehicle, variations in vertical lift must result in changes in the heading of the vehicle as trajectory control is achieved by roll modulation. Thus, it is of interest to examine minimum range entries for which, in addition to an acceleration constraint, the final cross range is constrained to zero.

A minimum range trajectory with zero cross range and with the acceleration dose constrained to a value of 1.0 is shown in figure 6(b). This trajectory can be compared with the similar minimum range trajectory of figure 6(a) for which cross range was not constrained. If the roll-angle variations are disregarded, the trajectories of figures 6(a)

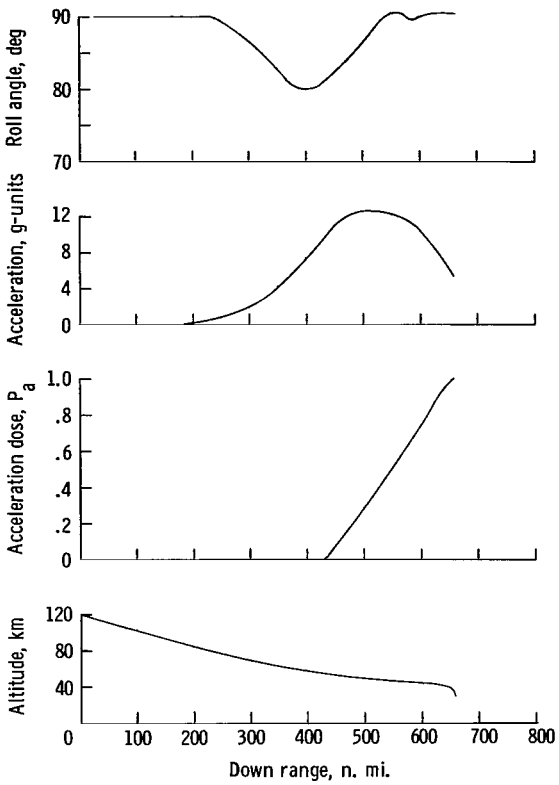

(a) Typical minimum down-range trajectory.

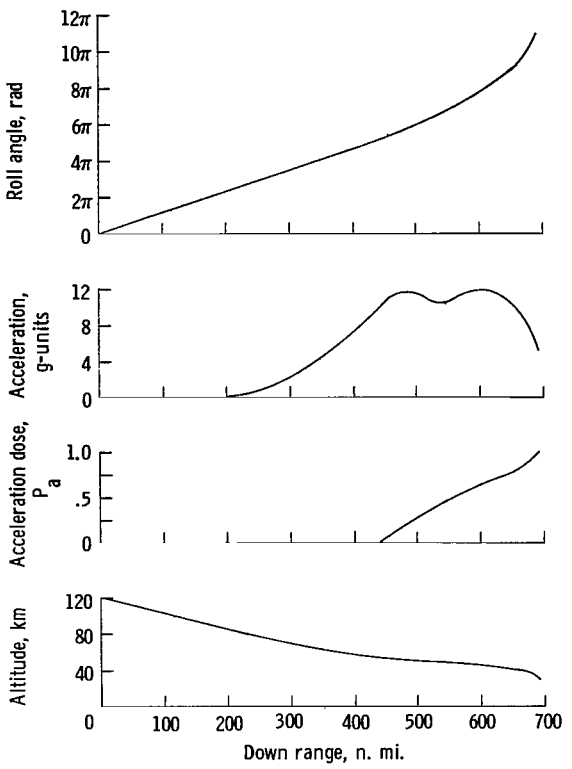

(b) Minimum down-range trajectory with final cross range constrained to zero.

Figure 6.- Effect of acceleration constraints on minimum down-range entries. V_0 = 10.972 km/sec; h_0 = 121.92 km; γ_0 = -6.5°; m/C_DS = 322 kg/m^2; L/D = 0.5.

and 6(b) are very similar, a penalty of about 40 nautical miles resulting from the cross-range constraint. However, the roll-angle history for the zero cross-range entry departs radically from that of figure 6(a) with a near-constant roll rate being employed during the entry. This roll rate maintains the cross range near zero throughout the entry. Thus, for straight-ahead minimum range entries, near-constant roll rates are used throughout the entry, the cross-range constraint causing small increases in minimum range.

The general effect on maneuver capability of varying the acceleration constraint is given in figure 6(c). This figure shows the minimum down range, peak heating rate, and peak acceleration of trajectories for which the acceleration dose was constrained to values between 0.2 and 1.0. Figure 6(c) shows that minimum down range is determined by the allowable acceleration dose and that the peak acceleration and peak heating rate decrease almost linearly as acceleration dose is reduced.

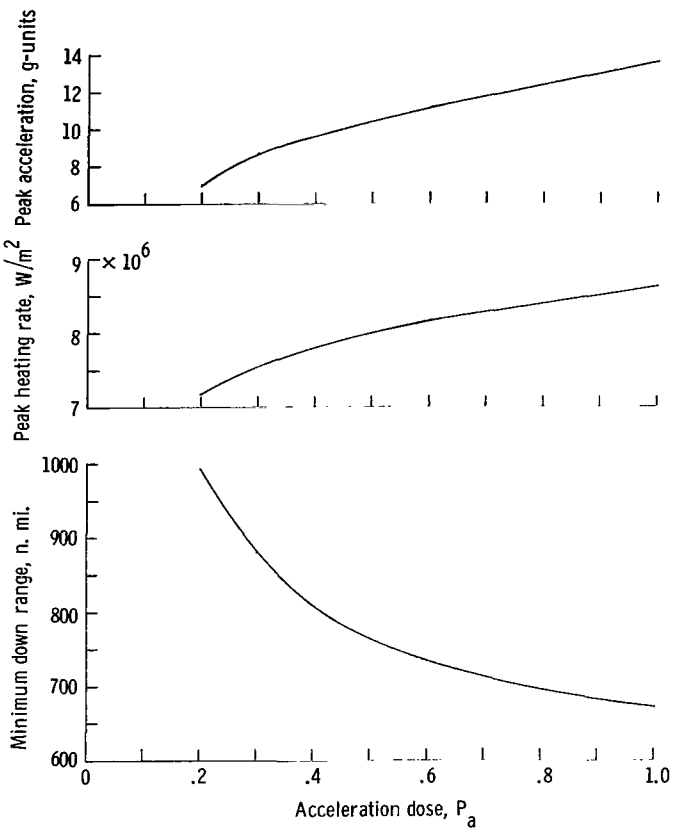

(c) General effect of acceleration constraints on minimum range.

Figure 6.- Concluded.

Although acceleration dose was used as the limiting factor in the data of figure 6(c), a related quantity would have been the peak heating rate. For short-range trajectories, the entry time is relatively small; thus, the total heat input is also small. However, the heating rates can become excessively high for these entries if no constraints are imposed. A constraint can be applied as a direct limit on heating rate or, as is shown in figure 6(c), can be indirectly achieved by limiting acceleration since acceleration and heating rate are closely related. Acceleration dose, rather than peak heating rate, was used in the present analysis since its use effected a more rapid convergence of the optimization procedure.

Effect of initial velocity on maneuver capability.- Results of previous sections of this report have been based on entry with an initial velocity of 10.972 km/sec (36 000 ft/sec). The effect on maneuver capability of variations in the initial velocity is now examined with the aid of figure 7.

Figure 7(a) gives typical maximum cross-range trajectories with initial velocities of 12.192 km/sec (40 000 ft/sec) and 9.754 km/sec (32 000 ft/sec). The down range for these entries was 2400 nautical miles and the initial entry angle was -6.5°. These trajectories can be compared with the similar trajectory of figure 4(a) which has an initial velocity of 10.972 km/sec. As expected, figures 7(a) and 4(a) show that the maximum cross range and convective heating increase as the initial velocity increases. The roll-angle histories for the three entries follow similar trends, the principal difference being that they are displaced such that more upward lift is used as the initial velocity is lowered. The flat portions in the roll-angle curves of figure 7(a) occur while the vehicle is outside the effective atmosphere and no control of the trajectory is possible.

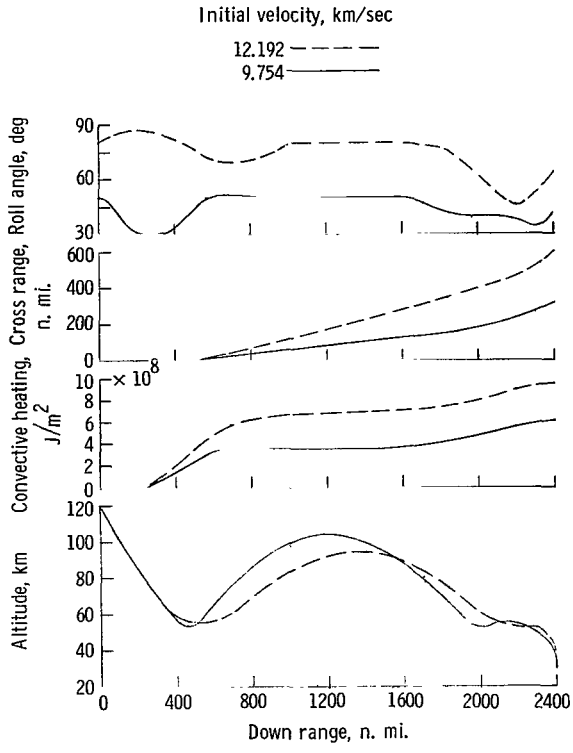

(a) Typical maximum cross-range trajectories with different initial velocities.

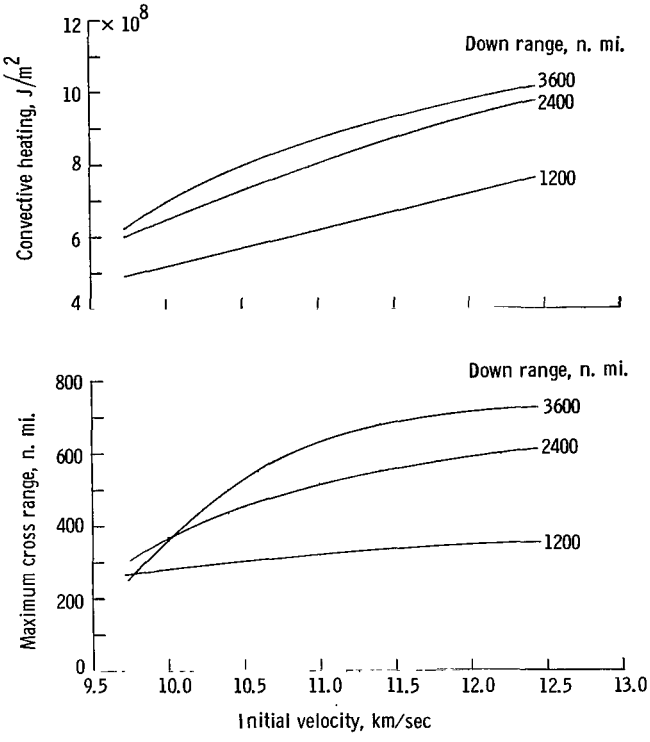

(b) General effect of initial velocity on maximum cross range and resultant convective heating.

Figure 7.- Effect of initial velocity on maximum cross range and resultant convective heating. h_0 = 121.92 km; γ_0 = -6.5°; m/C_DS = 322 kg/m^2; L/D = 0.5.

The general effect of initial velocity on maneuver capability and convective heating is given in figure 7(b) for three down-range conditions. Figure 7(b) shows, as did figure 7(a), that the maximum cross range, for a particular down range, increases as the entry velocity becomes larger. The convective heating is shown to vary almost linearly with initial velocity for each down-range condition. It is of interest to note that at the lowest initial velocity given in figure 7(b), the maximum cross range is smaller for the 3600-nautical-mile entry than for the 2400- or 1200-nautical-mile entries. This condition results since for the long-range low-velocity entry, most of the lift must be used in meeting the down-range constraint and, hence, little lift is available for lateral maneuvering.

Comparison of maximum maneuver capability with that obtained by use of typical entry guidance systems.- It is of interest to compare the results of the present analysis with those of previous studies in which the maneuver capability for Apollo-type vehicles was determined by using entry guidance systems based on analytic techniques as well as

systems for which a human pilot was included in the control loop. Although an accurate comparison is difficult because of differences in computational methods and assumptions, the general trend can be established for certain classes of entry missions. The present discussion is limited to trajectories for which no in-flight constraints are imposed since this type of entry offers the best basis for comparison. Thus, the following remarks are largely concerned with relating the results of figure 3 to data from previous studies.

Consider the results of reference 7 which were for a vehicle and mission similar to that of the present study and which were computed by using a reference trajectory type of automatic guidance system. These results, which include the maneuver capability for various entry conditions, compare with those of figure 3 as follows. For similar entry conditions, the maximum cross-range data of figure 3 are significantly greater than those of reference 7, the increases varying from about 15 percent for a down range of 2600 nautical miles to 30 percent for a range of 1300 nautical miles. The minimum range conditions shown in figure 3 are also found to be substantially reduced over those of reference 7, reductions of 200 nautical miles or more being realized. A comparison of figure 3 with similar results for pilot-controlled entry, such as are given in reference 8, yields the same general pattern as that for automatic guidance systems. Thus, although range capability results of the present analysis do not depart radically from those obtained with practical entry guidance systems, significant increases in maneuver capability can be realized with the optimal trajectories.

Further insight into the conclusions of the foregoing discussion can be achieved by comparing the nominal trajectories used to initiate the optimization process with the resulting optimal trajectories. The nominal trajectories generally used for maximum cross-range entries were computed with a constant roll angle such that the desired terminal constraint on down range was satisfied. For example, a constant roll-angle of 71° was used in establishing the nominal trajectory for the long range entry of figure 2. The increase in cross range for an optimal entry over that for the corresponding nominal trajectory was from 20 to 30 percent over the spread of conditions given in figure 3. This increase in cross-range capability is seen to compare favorably with that found when optimal data are contrasted with those obtained with other entry guidance schemes.

Optimization of Entry Heating

In this section the analysis departs from a direct consideration of terminal maneuver capability and various aspects of entry heating are investigated. The objective is to establish heating boundaries for various entry conditions and to show the effect of appropriate constraints on these boundaries. As previously described, the primary area of interest is convective heating. Nominal initial conditions are used unless otherwise specified.

Convective heating boundaries.- Lower and upper limits on entry heating were established by either minimizing or maximizing the heat input for various trajectory constraints. Typical minimum and maximum heat trajectories are given in figure 8 for entries with a down range of 1200 nautical miles.

The minimum and maximum or optimal heat trajectories shown in figure 8 are very different in nature. For the minimum heat trajectory, negative lift (roll angle > 90°) was initially used to force the vehicle into the dense atmosphere. As acceleration increased to a peak value of about 30g, the roll angle was rapidly reduced to zero and thus produced maximum upward lift. This lift caused the vehicle to exit the atmosphere and follow a ballistic path to the reentry point where a second acceleration pulse was encountered. The maximum heat trajectory of figure 8 consists of an initial pullup using maximum upward lift followed by a near-constant-altitude trajectory to the desired terminal point. In contrast to the sharp but high acceleration pulses for minimum heating, this maximum heat trajectory features low levels of acceleration throughout the entry. The steady increase in convective heating for this trajectory results in a 60-percent increase in heat input over that for the corresponding minimum heat trajectory.

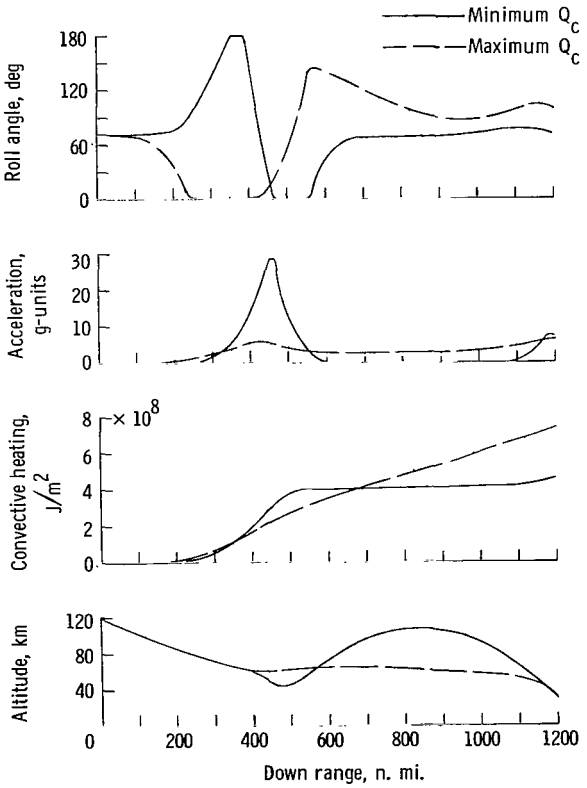

Figure 8.- Typical minimum and maximum convective heating trajectories. V_0 = 10.972 km/sec; h_0 = 121.92 km; γ_0 = -6.5°; m/C_DS = 322 kg/m²; L/D = 0.5.

An interesting feature of minimum and maximum heat trajectories is that for the same down-range condition, the entry time is considerably longer for a minimum heat entry than for the corresponding maximum heat entry. For example, with the entries given in figure 8, the minimum heat entry required 403 seconds whereas the maximum heat entry required only 290 seconds. This result occurs since the vehicle decelerates rapidly during the initial part of the minimum heat entry and then spends a large portion of the entry in near-ballistic flight at reduced velocity (V = 4.2 km/sec (13 780 ft/sec) at apogee of skip for entry in fig. 8).

An explanation for the minimum heating trajectory of figure 8 is found in reference 9, where it is shown that to achieve minimum heating, the vehicle maintains the highest Reynolds number consistent with the load limit and, hence, the lowest ratio of friction to pressure drag. Although, as shown in reference 9, the ideal lower boundary on convective

heating load would be provided by a constant maximum deceleration slowup, this result is not possible for entries with a down-range constraint. Thus, for these entries, the range constraint forces a compromise such that minimum heating is achieved by slowing down at the highest rate and earliest time possible and then by rapidly exiting from the atmosphere with just enough energy to attain the desired range. The determining factors behind the shape of the maximum heating curve of figure 8 are obvious. The vehicle merely attains and maintains the largest possible heating rate consistent with the down-range constraint. Therefore, although this heating rate may be less than that for other type trajectories, it is maintained at a near-constant value throughout the entry and thus increases the heat "soak-time."

Minimum and maximum heat trajectories for other down range conditions are similar to those given in figure 8. For longer ranges the minimum heat entries must naturally skip to higher altitudes, whereas the maximum heat entries must ascent into less dense atmosphere in order to meet the down-range constraints. However, in general, minimum heat trajectories are characterized by large initial acceleration pulses and ballistic skips (ref. 1) whereas maximum heat trajectories feature low-altitude low-acceleration flight paths.

A summary plot showing minimum and maximum heat boundaries for various down-range conditions is given in figure 9. The results given in this figure were obtained by either maximizing or minimizing entry heating with only a down-range constraint imposed. Thus, as is shown in later sections of this report, some of the trajectories on the minimum heating contour of figure 9 would be unrealistic from a manned mission standpoint because of the large acceleration peaks encountered for short ranges and the high skip altitudes which result for the longer range entries.

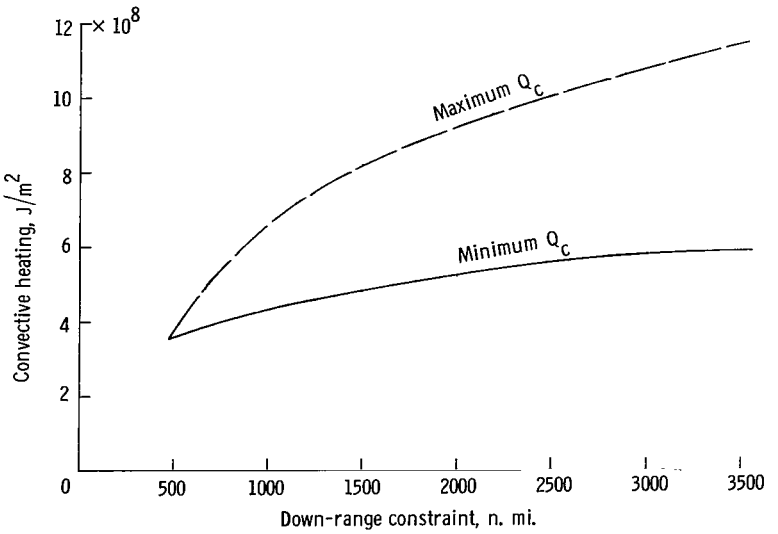

Figure 9.- Optimal convective heating boundaries for various down-range entries. V_0 = 10.972 km/sec; h_0 = 121.92 km; γ_0 = -6.5°; m/C_DS = 322 kg/m^2; L/D = 0.5.

In addition to giving boundaries on convective heating, figure 9 also provides other useful information. For example, consider an entry with the same initial conditions as figure 9 for which, because of heat-shield limitations, the total convective heat input could not exceed 5×10^8 J/m^2. Figure 9 shows that for these conditions the upper and lower limits on

down-range capability would be about 1700 and 500 nautical miles, respectively. Thus, for entries with an upper limit on heat input, the data of figure 9 give information on a vehicle's maximum maneuver capability or terminal footprint.

In the section "Maximum Maneuver Capability," a comparison was given between the nominal trajectories used to initiate the optimization procedure and the optimal trajectories which resulted. A similar discussion regarding the data of figure 9 is of value since it offers a possible standard for comparison of heating attained on typical entry trajectories with that achieved under optimal conditions.

As before, the nominal trajectories generally used for optimal heat entries were computed with a constant roll angle such that the desired terminal constraint on down range was satisfied. Thus, if points on the minimum or maximum boundaries of figure 9 were desired for a particular down-range condition, a constant roll-angle trajectory which gave this down range was used as the nominal. The optimal heat entries represented in figure 9 compared with the assumed nominal trajectories in the following manner. The heat input for a minimum heat trajectory was generally about 30 percent less than that for the corresponding nominal trajectory whereas the input for a maximum heat trajectory was about 20 percent greater than that for the corresponding nominal trajectory. For example, with a down range of 1800 nautical miles, the heat input for the nominal trajectory was 7.4×10^8 J/m^2. Thus, as shown in figure 9, a reduction of 31 percent was achieved by minimizing entry heating whereas an increase of 19 percent was realized for the maximum heating entry.

Effect of trajectory constraints on convective heating boundaries.- As previously described, minimum heat trajectories for relatively short range entries are characterized by high levels of peak acceleration. Thus, for these entries, acceleration constraints are advisable. Figure 10(a) shows the effect of an acceleration constraint on a typical minimum heat trajectory. For the entry given in this figure the down range was 1200 nautical miles and the acceleration dose was limited to a value of 1.0. For comparison purposes the unconstrained minimum heat trajectory of figure 8 is also given.

An examination of figure 10(a) shows that the acceleration constraint leads to a reduction in the initial acceleration peak of about 12g over that of the unconstrained entry. The acceleration constraint, in effect, also acts as an altitude constraint since it lowers the skip altitude by about 20 kilometers. This lower skip trajectory and smaller acceleration result in an increase of about 17 percent in convective heating as is shown by figure 10(a).

The overall effect of acceleration constraints on heating boundaries is given in figure 10(b) for various down-range conditions and a number of acceleration constraints. Shown also in figure 10(b) is the peak acceleration attained for each condition on the heat-boundary contours. As expected, this figure shows that reductions in the allowable acceleration dose result in increases in the minimum heating for corresponding down-range

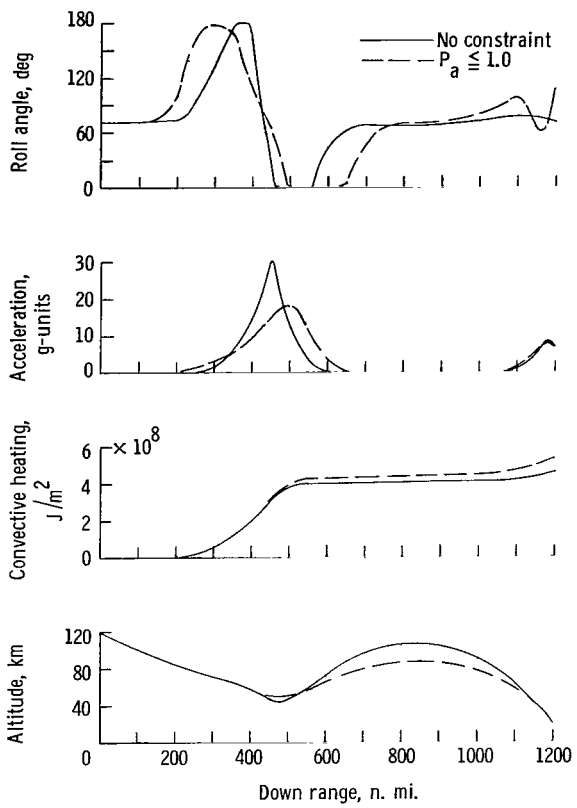

(a) Effect of acceleration constraint on typical minimum convective heating trajectories.

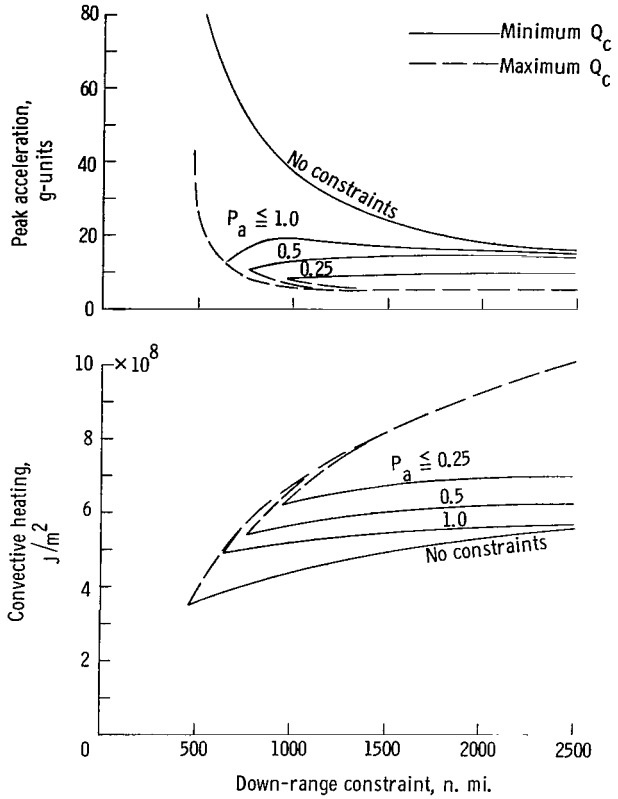

(b) General effect of acceleration constraints on optimal convective heating boundaries and on peak acceleration.

Figure 10.- Effect of acceleration constraints on optimal convective heating boundaries. V_0 = 10.972 km/sec; h_0 = 121.92 km; $\gamma_0 = -6.5^0$; m/C_DS = 322 kg/m^2; L/D = 0.5.

conditions. Also, for acceleration doses of about 0.5 or less, the maximum heat boundary is reduced for conditions near the lower limit on down range.

The acceleration curves of figure 10(b) show that for down ranges greater than about 1000 nautical miles, the peak acceleration attained is nearly constant for a specified level of acceleration dose. Thus the dose limit imposed acts indirectly to constrain peak acceleration to a particular level. It should be stated that this effect is not reversible. For example, if minimum heat trajectories were computed with a peak acceleration constraint imposed, the resulting acceleration dosage would not necessarily correspond to the levels shown in figure 10(b). The dose levels should, in fact, be generally higher than those given in figure 10(b) since minimum heating would probably be achieved by maintaining the acceleration at its upper limit for as long a time as is consistent with the down-range constraint.

Because of the inherent tendency of unconstrained minimum heat entries to follow skip trajectories, it is of interest to investigate the effect of an altitude constraint on these trajectories. This altitude-constraint effect will now be examined with the use of figure 11.

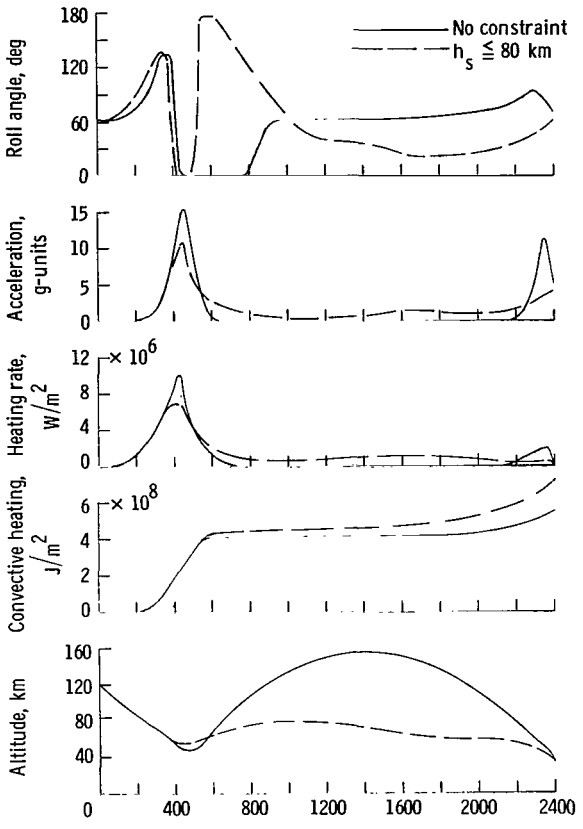

(a) Effect of altitude constraint on typical minimum convective heating trajectory.

Figure 11.- Effect of altitude constraints on optimal convective heating boundaries. V_0 = 10.972 km/sec; h_0 = 121.92 km; $\gamma_0 = -6.5^0$; m/C_DS = 322 kg/m^2; L/D = 0.5.

Typical minimum heat trajectories are given in figure 11(a) for entries with and without an altitude constraint. For the entries shown, the down range was 2400 nautical miles and in one entry the skip altitude was limited to 80 kilometers. The unconstrained trajectory of figure 11(a) is similar to that of figure 10(a), the skip altitude approaching 160 kilometers. On the altitude-limited trajectory, the vehicle pulls up more rapidly and then uses negative lift to reduce the flight-path angle to zero at the desired skip altitude. This lower altitude trajectory results in an increase in heating of about 30 percent over that for the unconstrained trajectory of figure 11(a).

The general effect of an altitude constraint on heating boundaries is given in figure 11(b). This figure gives the minimum and maximum heating attainable for various down-range conditions and altitude constraints. Also given is the skip altitude which results for trajectories on the unconstrained minimum and maximum heating contours. As is shown in figure 11(b), decreases in the skip-altitude constraint result in increases in minimum heating. The skip altitude also determines the maximum down range for an entry as is shown by the contours in figure 11(b) for which the skip altitude was limited to 60 km. Note that for the range of conditions included in figure 11(b), only the 60-km altitude constraint affects the upper limit on heating, the effect being a lowering of this boundary for ranges greater than about 1000 nautical miles.

The increased heating due to long range coast in the atmosphere as compared with skip trajectories, shown in figure 11(b), may not impose a proportional penalty on the heat shield. For example, with a charring ablator type of heat shield (refs. 10 and 11), a portion of the heat is dissipated by reradiation. Thus, the longer duration heat pulses achieved on altitude-limited entries (fig. 11(a)) may result in a greater percent of the total heat input being dissipated by reradiation. Since this ablation effect could not be included in the present study, a possible need exists for more refinement in the future studies in representing the properties of ablating materials.

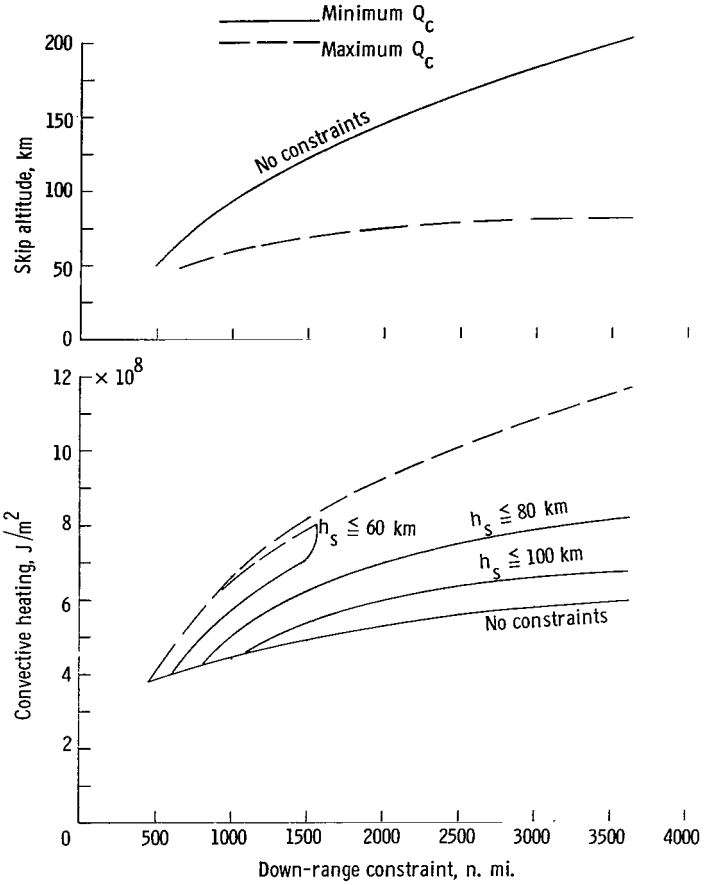

(b) General effect of altitude constraints on optimal convective heating boundaries.

Figure 11.- Concluded.

The data of figure 11(b) can also be interpreted in a manner similar to that which was given in the discussion of figure 9. For example, consider entries for which, because of vehicle and mission requirements, the skip altitude must remain below 80 kilometers and the total convective heat load must not exceed 7.5×10^8 J/m^2. For these conditions figure 11(b) shows that the maximum down range attainable is 2500 nautical miles and, if acceleration is not limited, the minimum range is about 500 nautical miles. However, in addition to the heating and altitude constraints, assume that the acceleration dose must not exceed a value of 0.25 which, as is shown in figure 10(b), would limit peak acceleration to about 10g. For this acceleration constraint, figure 10(b) shows that the minimum down range would be about 950 nautical miles. A further check must be made to assure that the maximum and minimum range conditions given are consistent with all the heating, altitude, and acceleration constraints. By referring to figures 11(b) and 10(b), it is seen that the maximum down range condition results in an acceleration dose smaller than the limit of 0.25 and the minimum range entry has a skip altitude below the 80-kilometer limit. Therefore, for the assumed constraints, the maneuver capability of the vehicle is between 950 and 2500 nautical miles. Thus, as has been shown in a previous example, the heating boundary results presented can be used to establish upper and lower limits on range capability.

Effect of initial entry conditions on convective heating boundaries.- Previous heating results were only for cases with nominal values for the initial entry conditions (V_O = 10.972 km/sec, γ_O = -6.5°). The effect on entry heating of variations in the initial entry conditions is now considered. Typical trajectories for various entry velocities and entry angles are not given as they are similar in nature to those previously shown in figures 10(a) and 11(a) for nominal entry conditions.

The effect of changes in the entry angle on minimum and maximum convective heating is given in figure 12. This figure, which is for a nominal velocity of 10.972 km/sec, shows the effect on heating of varying the entry angle from about -5.5° to about -7.5° for a number of down-range conditions. Also shown in the figure is the peak acceleration and the peak heating rate attained for each entry. Over the range of conditions given in figure 12, both the upper and lower bounds on heating increase almost linearly as the entry angle becomes shallower. The figure also shows, as could be expected, that the peak acceleration and peak heating rate for minimum or maximum heating is reduced as the entry angle is reduced. Only one acceleration curve and one heat-rate curve are given on the maximum boundary since they are almost independent of range for the conditions shown in figure 12.

One might expect that the inverse relationship between heating and entry angle results from the longer flight times that could be expected for the shallower entry angles. However, this is not the case as, for a particular down range, the entry time actually increases as the entry angle becomes steeper since the vehicle achieves its maximum acceleration early in the entry and spends more time in the ballistic skip at a reduced velocity. The increase in heating with reduced entry angle, shown in figure 12, in reality results from the smaller and broader acceleration pulse (or heat-rate pulse) attainable as entry angle is decreased. This effect can also be seen by referring to figure 10(b) which shows that, for a specific down range, lowering the peak acceleration increases the minimum heat input. The increase in the upper bound on heating with reduced entry angle results from a similar acceleration effect as can be seen by referring again to figure 10(b). Thus, for minimum or maximum heat trajectories with a specific initial velocity and down range, reductions in the initial entry angle lead to reductions in peak acceleration and peak heating rate which, in turn, result in an increase in the minimum and maximum heat boundaries.

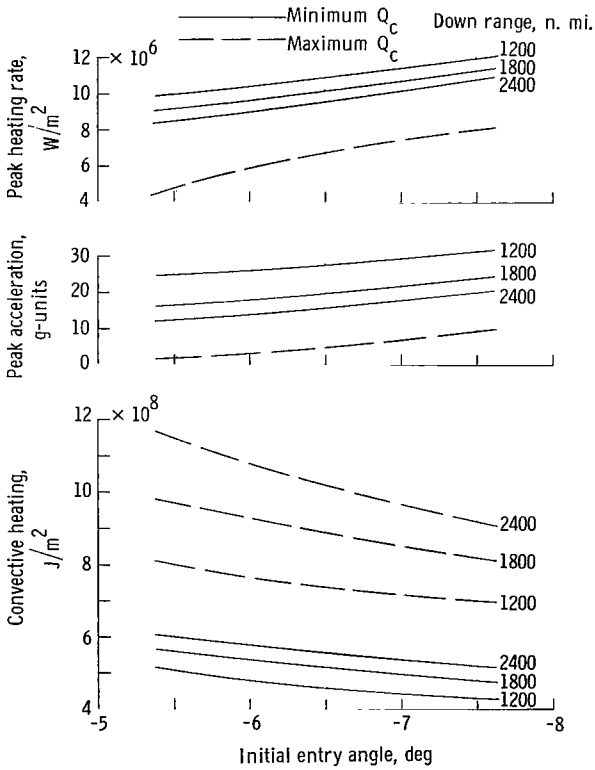

Figure 12.- Effect of entry angle on optimal convective heating boundaries. V_0 = 10.972 km/sec; h_0 = 121.92 km; m/C_DS = 322 kg/m^2; L/D = 0.5.

The effect on optimal heating of varying the initial entry velocity is shown in figure 13. Given in this figure is the

minimum and maximum convective heating attainable for various down-range conditions with initial velocities between about 9.5 and 12.5 km/sec. Also given are the peak acceleration and the peak heating rate attained for each entry condition.

Figure 13 shows that the boundaries on convective heating are raised as the initial velocity is increased. This result is to be expected since convective heating is a strong function of velocity ($Q_c \propto V^3$). Thus, as initial velocity is increased, more energy must be dissipated during the entry and, therefore, total heat input increases. Note that, while peak acceleration increases with increasing velocity as shown in figure 13, this is not the predominant factor in determining minimum entry heating as for the data of figure 12 for which all entries were with the same initial velocity and energy. Note also that, for maximum heat entries, peak heating rate increases with increasing velocity whereas the reverse is true for peak acceleration. This effect results since, as initial velocity is increased, the greater lift and centrifugal force on the vehicle permit a pullout at a higher altitude. Thus, peak acceleration is reduced while, because of the strong dependence of heating on velocity, the heating rate increases.

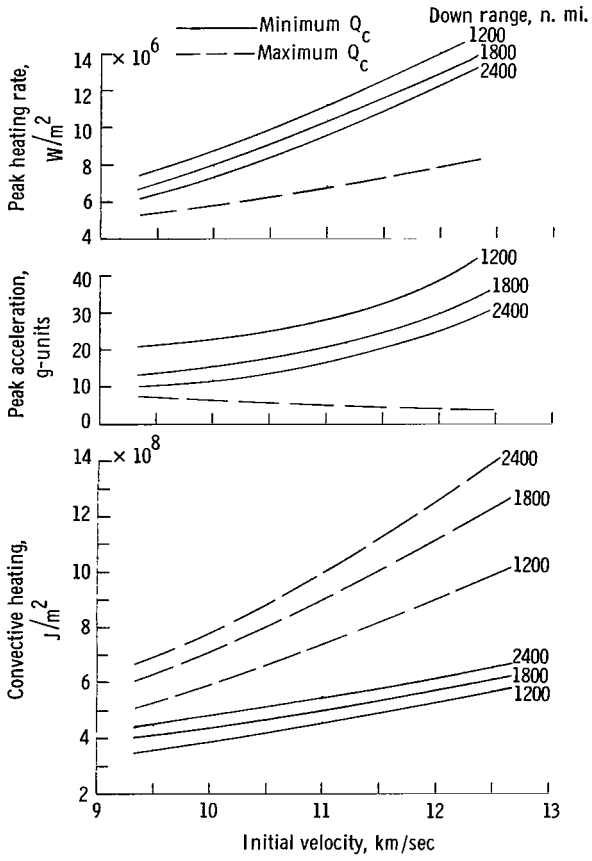

Figure 13.- Effect of entry velocity on optimal convective heating boundaries. h_0 = 121.92 km; γ_0 = -6.5°; m/C_DS = 322 kg/m²; L/D = 0.5.

With reference to figures 12 and 13, an additional heating effect is of interest. Although both the lower and upper bounds on heating increase with decreasing entry angle (for V_0 = Constant) or with increasing entry velocity (for γ_0 = Constant), the change in the upper boundary is proportionately larger than that for the lower boundary. Thus, the spread of heating values is widened as entry angle is reduced or as entry velocity is increased. For example, consider entries with a down range of 2400 nautical miles. From figure 12 it is seen that reducing the entry angle from -7.5° to -5.5° increases the lower heat boundary by about 0.8×10^8 J/m² whereas the upper boundary is increased by about 2.3×10^8 J/m². Thus, for the assumed conditions, a reduction in entry angle of 2° leads to an increase in the width of the heating boundaries of nearly 40 percent. This heat-boundary effect is even greater when entry velocity is increased, as is shown by figure 13. For example, with a down range of 2400 nautical miles, increasing

the entry velocity from 10 km/sec to 12 km/sec increases the width of the heat boundary by over 100 percent.

It is reassuring to note that the heating rates shown in figures 12 and 13 are in general agreement with those given in reference 10 for the Apollo vehicle.

Radiative Heating Effects

Previous results on entry heating have included only the convective contribution to entry heating. Brief consideration is now given to radiative heating and its effect on optimal heat trajectories. As described in the section "Scope of Study," the heating calculations are based on assumed empirical models for radiative heating and the results presented should be considered with reference to these assumptions. Although the results would have varied somewhat if other heating models had been used, they are considered to be representative of the stagnation radiative and convective heating which would occur during entry with the assumed initial entry conditions and vehicle.

Given in figure 14(a) are minimum heating trajectories for which only radiative effects are included and for which both radiative and convective contributions were considered. A comparison of the minimum total heat trajectory of figure 14(a) with a similar trajectory given in figure 8 for which only convective heating was included shows that, except for a slight increase in peak acceleration and about a 10-percent rise in heat input for the total heat entry, the two trajectories are similar. This condition results since the radiative contribution to the total heat is small compared with the convective contribution as is also shown by the relative low level of heating attained for the radiative heating trajectory in figure 14(a).

Although total heating and convective heating trajectories are nearly identical, the minimum radiative heat trajectory of figure 14(a) departs radically from other types of minimum heating entries. This trajectory, in fact, is similar in nature to that for maximum convective heating as a comparison of figures 14(a) and 8 shows.

Typical entries for which radiative heating as well as total heating were maximized are given in figure 14(b). These results, which were for a down range of 1200 nautical miles, can be compared with the trajectory in figure 8 for which convective heating was maximized. As for minimum heating, the maximum total heat entries differ little from those for which only convective heating was included. It is of interest to note that the maximum radiative heat trajectory given in figure 14(b) is similar to the minimum convective heat results given in figure 8.

Optimal radiative and total heat entries were computed for other down range conditions and the results were in agreement with those of figures 14(a) and 14(b). Thus, for entry velocities of about 11 km/sec, although equilibrium radiation contributes about 10 percent to the total heat input, the shape of optimal heat trajectories is largely

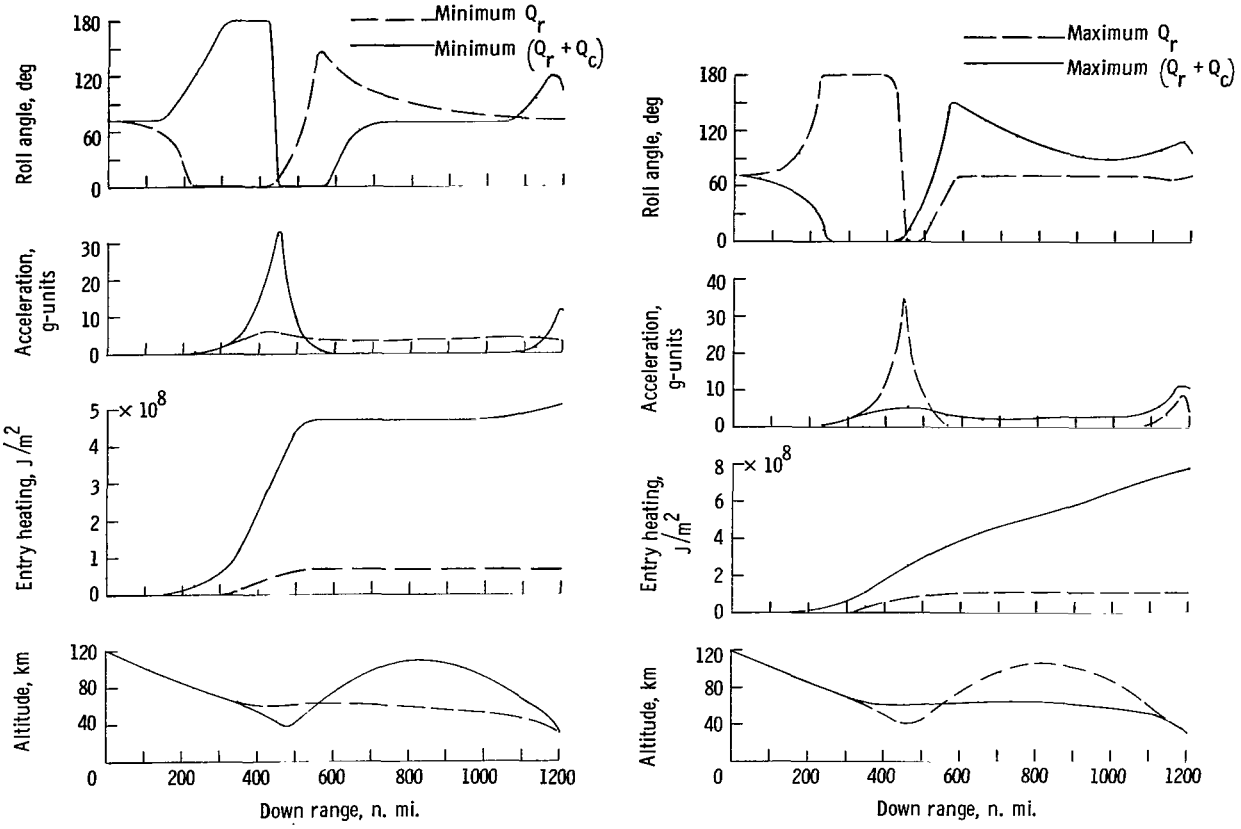

(a) Typical minimum heating trajectories comparing radiative and convective inputs.

(b) Typical maximum heating trajectories comparing radiative and convective inputs.

Figure 14.- Effect on optimal heating entries of including equilibrium radiation effects. V_0 = 10.972 km/sec; h_0 = 121.92 km; γ_0 = -6.5°; m/C_DS = 322 kg/m^2; L/D = 0.5.

determined by convective inputs. Also, minimum radiative heat trajectories tend to follow the same shape as maximum convective heat trajectories whereas maximum radiative heat entries are similar to those for minimum convective heating.

Minimum radiative and total heat entries were also computed for entry velocities above and below the nominal value of 10.972 km/sec. For smaller velocities the radiative effects were naturally less than those shown in figures 14(a) and 14(b) and, thus, could be neglected for all practical purposes. For entry velocities greater than 10.972 km/sec radiative contributions were, of course, found to be of increasing importance. For example, with an entry velocity of 11.6 km/sec, radiative heating accounted for almost 25 percent of the total heat input. However, optimal heat trajectories at this entry velocity were still strongly dominated by convective heating and continued to follow the general shape of optimal entries for which only convective heating was included. Optimal total heat entries with velocities in excess of 11.6 km/sec were not considered since above

this velocity, the constants in the radiative heat equation change values (ref. 4), and no provisions for accomplishing this change were included in the optimization program.

As shown in reference 4, for entry velocities of about 12.2 km/sec, radiative inputs are of near equal importance to convective inputs; thus, for these velocities optimal heat trajectories could be expected to assume some compromise shape between those given in figures 14(a) and 14(b). However, since radiative heating is basically a high-velocity effect which occurs during the early part of a trajectory and which cannot be controlled as easily as convective heating, it could be expected that even for entry velocities around 12 km/sec (39 370 ft/sec), the general shape of optimal total heat trajectories would continue to be dominated by convective effects. An obvious need for further study exists in this high-velocity region of the entry corridor.

Correlation and Trade-Off Between Maximum Maneuver Capability and Optimal Heating

The previous analysis has investigated trajectories for which either range or heating was optimized separately subject to in-flight constraints on altitude or acceleration. The combined effects of optimal heating and maneuver capability are now considered with the objective of finding a possible trade-off between these quantities.

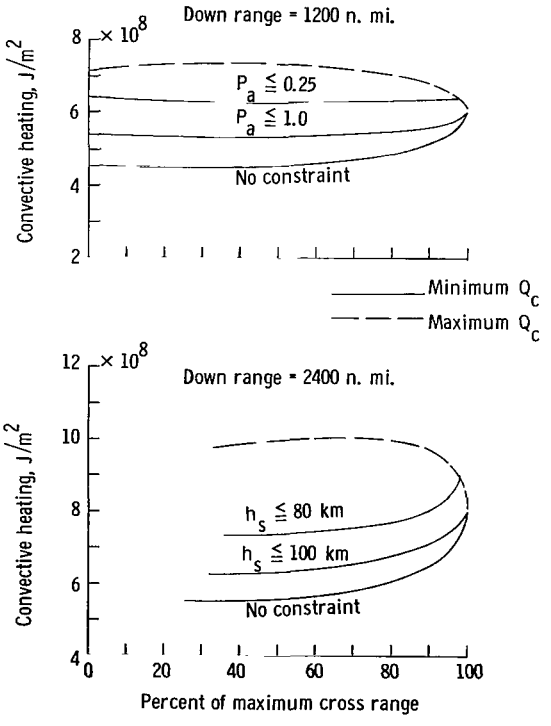

Figure 15.- Trade-off between maximum maneuver capability and optimal convective heating. V_0 = 10.972 km/sec; h_0 = 121.92 km; $\gamma_0 = -6.5^0$; m/C_DS = 322 kg/m^2; L/D = 0.5.

Given in figure 15 are summary plots of two down range conditions for which cross range was constrained to various values up to its maximum and for which convective heating was either minimized or maximized. Acceleration constraints are included for the short-range condition of 1200 nautical miles and altitude constraints were applied for the 2400-nautical-mile entries. The 100 percent of maximum cross-range points given in figure 15 correspond to the entries for which cross range was maximized, and the minimum and maximum points on the curves refer to entries for which heating was either minimized or maximized with only a down-range constraint included in each case.

As is shown in figure 15, the minimum heating curves are reasonably flat over much of cross-range capability, the large increase in heating occurring as the maximum cross-range condition is approached. For example, consider unconstrained entries, with a down

range of 2400 nautical miles. Figure 15 shows that, although the minimum heating condition corresponds to only about 30 percent of the maximum cross range, about 80 percent of the increase in heating with cross range occurs in the last 20 percent of maximum cross-range capability. Thus, by reducing the maximum cross-range requirements by 20 percent, a large reduction in entry heating can be achieved. This effect is also true for the unconstrained, short-range entries given in figure 15 and to a somewhat smaller extent for the altitude-limited and acceleration results given. For the results shown in figure 15, the absolute minimum heating condition occurred in the range between 20 and 40 percent of maximum cross range. It is therefore of interest to note that the heating levels increased only slightly as the cross range was reduced to zero. Thus, no significant heating penalty is incurred for "straight ahead" entries. This result could be expected for a vehicle with a capability for varying lift in the vertical plane (by varying angle of attack) without affecting lateral lift but might not be anticipated for the assumed fixed-lift-drag-ratio vehicle which achieved lift variation by roll modulation. Since the resulting trajectories for these zero-cross-range entries are of an interesting nature, a typical trajectory for this type of entry is given in figure 16.

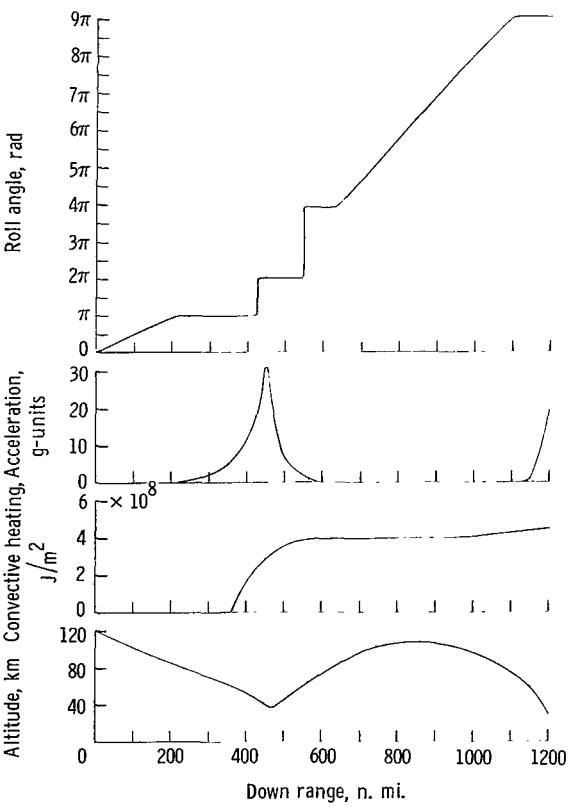

Figure 16.- Minimum convective heating trajectory with final cross-range constrained to zero. V_0 = 10.972 km/sec; h_0 = 121.92 km; γ_0 = -6.5°; m/C_DS = 322 kg/m²; L/D = 0.5.

Figure 16 shows a minimum convective heating trajectory with a down range of 1200 nautical miles for which the final cross range was constrained to zero. The roll-angle history for this entry follows an interesting pattern. Preceding the initial acceleration buildup, the vehicle rolls to direct lift downward as was the case for previous minimum heating entries (fig. 8). As the acceleration peak was approached, a near step input in roll angle was employed to position the vehicle such that lift was directed in an upward direction. During the ascent into less dense atmosphere, the vehicle rolled rapidly through 360° and again assumed an upward lifting condition. This last roll maneuver probably resulted from the initial reference trajectory used, which was a constant roll rate of 290° per minute (this roll rate resulted in a down range of 1200 n. mi. and very little cross range), since it allowed the vehicle to employ this reference roll rate while outside the

atmosphere. As the vehicle re-entered the atmosphere, it assumed a downward lifting position throughout the remainder of the entry, as is shown in figure 16.

Minimum heating trajectories for straight-ahead entries with other down-range conditions and with acceleration and altitude constraints imposed were similar to those shown in figure 16. Thus, to achieve minimum heating with no final cross range, a near bang-bang type of control is used such that lift is directed only in the vertical plane during critical portions of the entry

Effect of Vehicle Characteristics on Optimal Performance

Previous results have been based on an entry vehicle with a lift-drag ratio of 0.5 and a ballistic parameter m/C_DS of 322 kg/m^2. The effect on optimal maneuver capability and heating of changes in the assumed vehicle characteristics is now considered with reference to results of figure 1. The effect of variations in the lift-drag ratio and ballistic parameter is included.

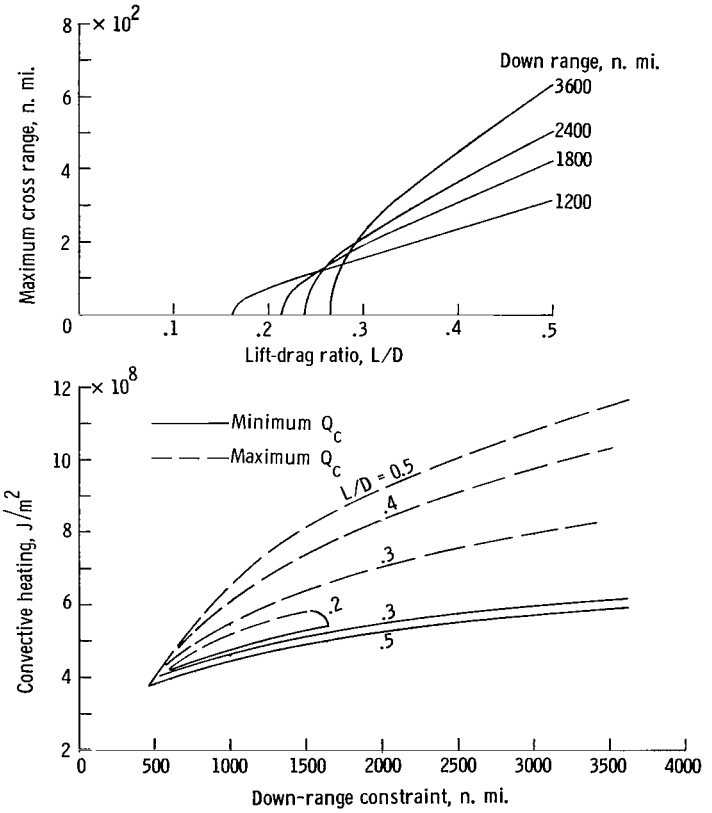

(a) Effect of variations in lift-drag ratio. $m/C_DS = 322$ kg/m^2.

Figure 17.- Effect of changes in vehicle characteristics on maximum maneuver capability and optimal convective heating boundaries. $V_0 = 10.972$ km/sec; $h_0 = 121.92$ km; $\gamma_0 = -6.5^0$.

Effect of changes in lift-drag ratio.- The effect on maximum maneuver capability and optimal heating of varying the lift-drag ratio of the assumed entry vehicle from about 0.2 to 0.5 is given in figure 17(a). Nominal entry conditions and a ballistic parameter of 322 kg/m^2 were used in obtaining these results.

For each down-range condition given, figure 17(a) shows that maximum cross range increases almost linearly with L/D over a large portion of the L/D variation considered. The zero cross-range condition shown for each down range corresponds to the smallest value of L/D for which that particular down range can be achieved.

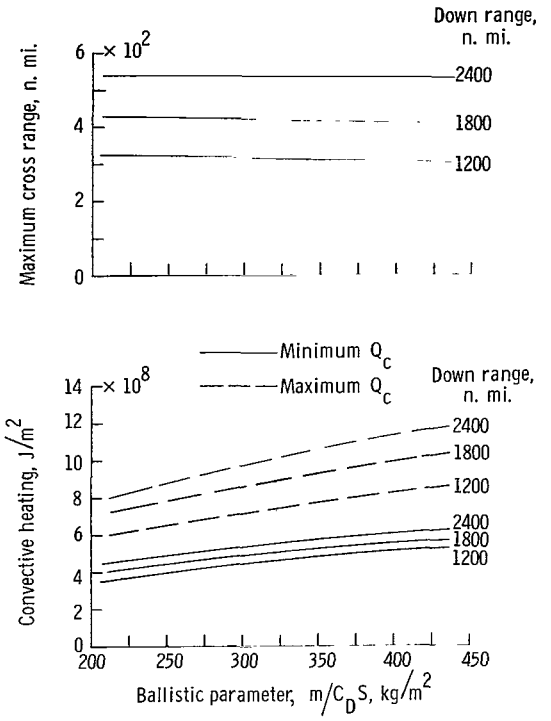

(b) Effect of variations in ballistic parameter m/C_DS. L/D = 0.5.

Figure 17.- Concluded.

The optimal heating data given in figure 17(a) show that the width of the convective heating boundaries is reduced as the lifting capability of the vehicle is lowered. This reduction in the width of the heating boundaries with reduced L/D results from a slight increase in the lower bound on heating as well as a proportionally larger decrease in the upper boundary, as is shown in figure 17(a). For example, with a down range of 2500 nautical miles, lowering the vehicle L/D from 0.5 to 0.3 raises minimum heating by only 5 percent whereas it lowers maximum heating by 25 percent. Thus, although reductions in the L/D of the vehicle lead to small increases in the lower boundary on heating, the relatively larger decreases in the upper boundary may make the overall effect a beneficial one from the viewpoint of entry heat protection. However, since reductions in lift requirements place a heavy penalty on maximum maneuver capability, trade-offs exist between vehicle lift-drag ratio, maneuver capability, and entry heating.

Effect of changes in ballistic parameter.- The effect on maximum maneuver capability and optimal heating of varying the ballistic parameter of the entry vehicle between about 200 and 450 kg/m^2 is given in figure 17(b). Nominal entry conditions and a lift-drag ratio of 0.5 were used to obtain these results.

Over the range of conditions given, figure 17(b) shows that variations in the ballistic parameter of the vehicle have only a small effect on the maximum cross range attainable. As is shown in the figure, the maximum cross range increases very slightly as the ballistic parameter is reduced. Figure 17(b) also shows that for a particular down-range constraint, minimum and maximum convective heating increase linearly with increases in the ballistic parameter. Thus, for the range of conditions included in the analysis, reductions in the ballistic parameter of an entry vehicle are beneficial from the point of view of both entry heating and maximum maneuver capability.

Effect of Rotation of Earth on Maximum Maneuver Capability and Optimal Entry Heating

The results given in previous sections of the report were obtained with the assumption of a nonrotating earth and atmosphere. Although the effect of the earth's rotation on maneuver capability and heating can be predicted intuitively, a limited number of results relating to this effect are included for completeness. The results to be presented were obtained for entries with an inertial velocity of 10.972 km/sec and a flight-path angle of -6.5°. Entries were assumed to be initiated at the equator with various inertial headings.

Entries with inertial headings along equator.- The effect on minimum and maximum convective heat boundaries of equatorial entries to the east and to the west is shown in figure 18(a). Also given is the peak acceleration achieved for each entry condition as well as the corresponding heating and peak acceleration resulting on similar entries for which the rotation of the earth was not included.

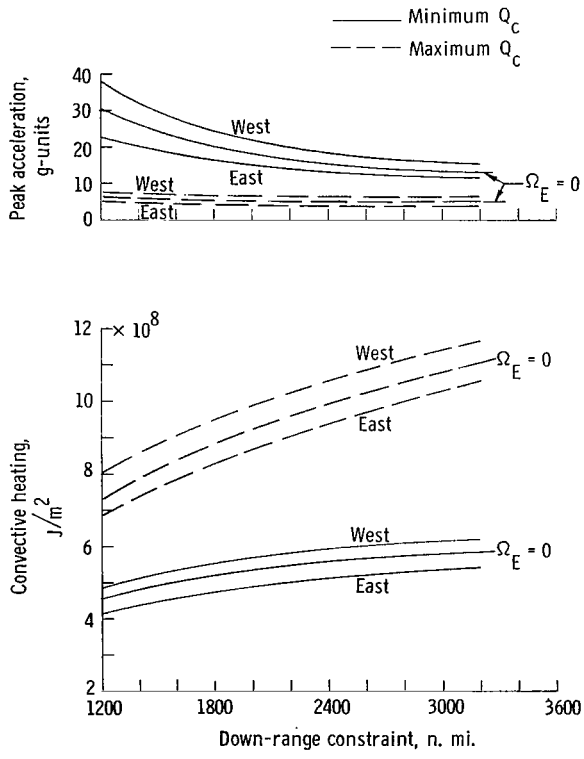

(a) Effect on heating boundaries and peak acceleration of initial headings toward east and west.

Figure 18.- Effect of earth's rotation on maximum maneuver capability and optimal convective heating boundaries. $V_{i,o}$ = 10.972 km/sec; h_o = 121.92 km; γ_o = -6.5°; $m/C_D S$ = 322 kg/m^2; L/D = 0.5.

The higher levels in minimum and maximum heating shown in figure 18(a) for western as compared with eastern entries are basically a velocity effect. This fact can be verified by referring to figure 13 which gave the effect of initial velocity on minimum and maximum heating for the case of a nonrotating earth. Consider minimum heating entries with a down range of 1200 nautical miles. An inertial velocity of 10.972 km/sec (36 000 ft/sec) results in initial velocities of about 10.5 and 11.44 km/sec, respectively, for eastern and western entries. Figure 13 shows that, for a down range of 1200 nautical miles, initial velocities of 10.5 and 11.44 correspond to minimum heating levels of 4.2×10^8 J/m^2 and 4.9×10^8 J/m^2; these values are in close agreement with the heating values given in figure 18(a) for similar conditions.

Trajectories were also computed to determine the effect on maximum cross range of initial headings to the east and west. Two factors influence the cross range for

these entries. The increased velocity for western compared with eastern entries tends to increase the maximum cross range, and the shorter range actually traveled for western entries (due to earth's rotation) tends to decrease the cross range. For example, with a desired down range of 2400 nautical miles, the actual ground distances traveled to the east and west were about 2580 and 2220 nautical miles, respectively, whereas for a down range of 1200 nautical miles, the distances were about 1320 and 1080 nautical miles, respectively. The data of figures 3 and 7(b) can be combined to show that these velocity and range effects could be expected to result in a slight increase (10 to 20 n. mi.) in maximum cross range for east-west entries as compared with the case for a nonrotating earth. The actual results obtained on east-west entries for which cross range was maximized were in general agreement with the previous predictions. However, since the differences in maximum cross range for the same down range were small between east, west, and nonrotating earth entries, the maximum cross range can for all practical purposes be taken to be constant for these entry conditions.

Thus, in summary, although velocity effects lead to increases in optimal heating levels for western equatorial entries over those for similar entries into a nonrotating atmosphere and although the reverse is true for eastern equatorial entries, velocity and earth-rotation effects on cross range tend to cancel for eastern and western entries and lead to near-constant values for maximum cross range for similar east, west, or nonrotating earth entries.

Entries with inertial heading toward north and south.- Since the rotation of the earth has only a small effect on a vehicle's velocity with respect to the atmosphere for north or south entries from the equator (increases it from 10.972 to about 10.974 km/sec), it would be expected that heat boundaries for these trajectories would be about the same as those for nonrotating earth entries. This result was found to be the case, as no apparent differences in optimal heating resulted between north, south, or nonrotating earth entries. However, as expected, the earth's rotation significantly influences the maximum maneuver capability for north-south entries as is shown in figure 18(b).

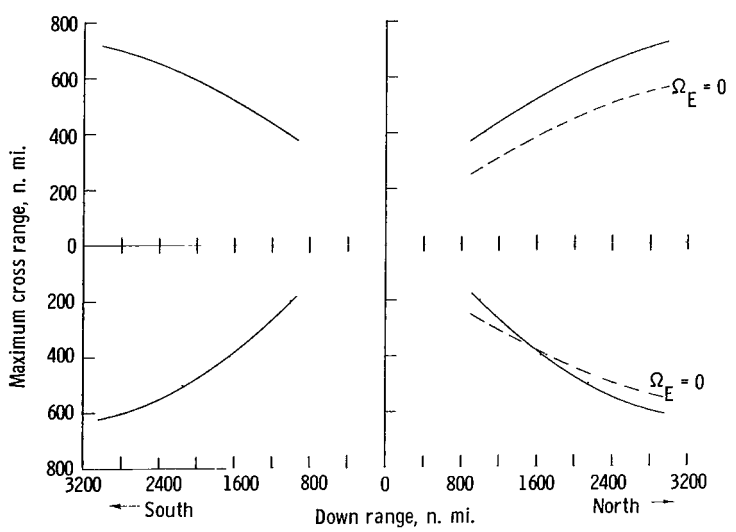

(b) Effect on maneuver capability of initial headings toward north and south.

Figure 18.- Concluded.

Given in figure 18(b) are the maximum cross ranges attainable, for a number of down-range conditions, for entries initiated at the equator into a rotating atmosphere with inertial headings toward the north and south. For comparison purposes, corresponding curves for nonrotating earth entry are also shown. Although previously given footprints, for which no earth rotation is included, are symmetrical about the down-range axis (dashed lines in fig. 18(b)), this is not the case for north-south entries as is shown in figure 18(b). This condition results from a combination of two factors. On north or south entries, for which the heading change is toward the east, the rotation of the atmosphere tends to aid in this heading change and hence the cross range is increased whereas the rotation of the earth beneath the vehicle tends to reduce the cross range. On north-south entries with heading changes toward the west, these atmospheric and earth-rotation effects tend respectively to reduce and increase cross range. The net effect, as is shown in figure 18(b), is that maximum cross range is greater for north or south entries with final destinations toward the west than for similar entries with heading changes to the east. Thus, as expected, the rotation of the earth under the vehicle is the dominant factor in determining maximum cross range for north or south entries.

For down ranges greater than about 1700 nautical miles, the maximum cross range is slightly greater for north-south entries with a rotating earth than for similar entries with a nonrotating earth. Thus, for these entries the increased heading changes resulting from the atmosphere's velocity component more than compensate for the reduction in cross range due to the rotation of the earth.

Optimization of Skip Trajectories

As was previously described, direct optimization of skip-type trajectories was found to be impractical because of the long computing times involved and due to convergence problems caused by the extreme dependence of terminal conditions on control inputs during the initial atmospheric phase of the entry. It is, however, possible to investigate certain portions of skip trajectories without considering the trajectory in its entirety. This approach is employed in the following discussion.

Given in figure 19(a) are optimal trajectories from a convective heating sense, for which the exit velocity and flight-path angle were constrained, respectively, to values of 7.772 km/sec (25 500 ft/sec) and 2^{o} at a skip altitude of 91.44 kilometers (300 000 ft). These skip conditions result in the vehicle traveling a distance of 6000 nautical miles in a ballistic trajectory from the exit altitude to a reentry point at the same altitude. Although the complete trajectory, which includes these exit conditions, is not optimal, the portion leading up to exit from the atmosphere, shown in figure 19(a), is of interest since it contrasts minimum and maximum heat trajectories for this phase of a possible skip entry.

A comparison of the roll-angle variations of figure 19(a) with previous optimal heat trajectories shows that the control inputs are similar during the initial entry phase. In general, figure 19(a) shows that for minimum heating, the vehicle pulls up rapidly after an initial high acceleration period and then uses negative lift to reduce the flight-path angle to the desired value at exit whereas for maximum heating, the vehicle decelerates more slowly and gradually increases the flight-path angle to the required value of 2^{o} at exit.

The distance traveled during the maneuvers shown in figure 19(a) was about 1000 nautical miles. Including the ballistic range of 6000 nautical miles and the reentry range of about 600 nautical miles gives an overall range of about 7600 nautical miles for this skip entry. The data of figure 9 could be extrapolated to predict a minimum heating level of at least 6×10^{8} J/m^{2} for an entry with this range. The minimum

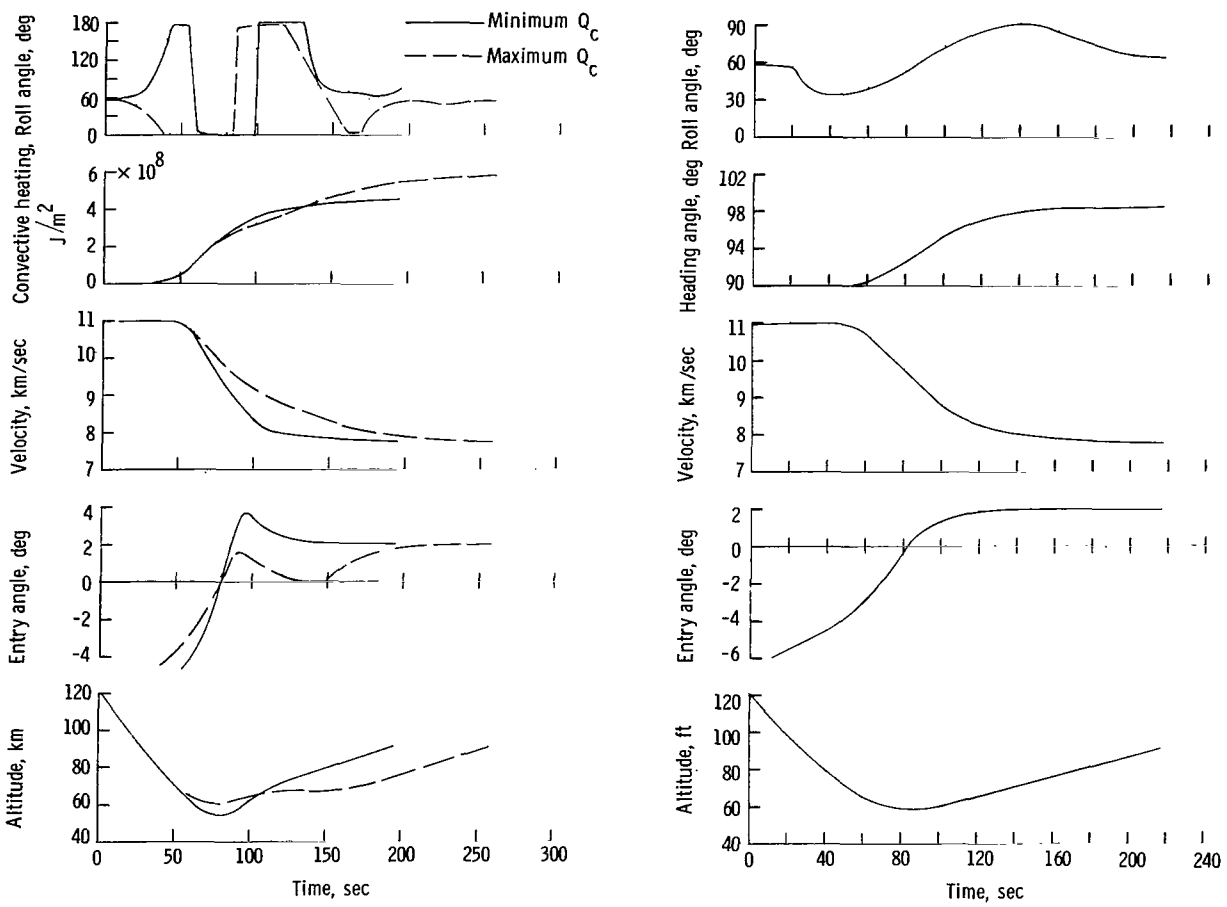

(a) Optimal convective heating.

(b) Maximum heading change.

Figure 19.- Initial atmospheric phase of typical optimal skip trajectories. V_0 = 10.972 km/sec; h_0 = 121.92 km; γ_0 = -6.5°; m/C_DS = 322 kg/m^2; L/D = 0.5; V_X = 7.772 km/sec; h_X = 91.44 km; γ_X = 2°.

heat level of 4.5×10^8 J/m^2 shown in figure 19(a) might appear to be inconsistent with this value. However, the minimum heating which can be achieved during the final reentry following the ballistic flight (V_o = 7.772 km/sec (25 500 ft/sec), h_o = 91.44 km (300 000 ft), $\gamma = -2^o$) is about 2×10^8 J/m^2 (1.76×10^4 Btu/ft^2). Hence, the total heat input for this skip entry of about 6.5×10^8 J/m^2 (5.73×10^4 Btu/ft^2) is in agreement with the results of figure 9 and shows that for ranges greater than about 3000 nautical miles, the increase in minimum heating with range is small.

An additional skip trajectory which could be of practical importance is given in figure 19(b). Shown here is the initial portion of a skip trajectory for which the change in vehicle heading was maximized subject to the same exit conditions as were imposed on the trajectories of figure 19(a). Figure 19(b) shows that a maximum heading change was achieved by applying a large part of available lift in a lateral direction throughout the entry and by using vertical lift to establish the desired exit flight-path angle early in the pullup phase. Although the resulting heading angle change of 8^o may not appear overly impressive, it becomes so when compared with the heading changes of about 2^o which resulted during the optimal heat trajectories of figure 19(a).

Guidance Sensitivity Requirements for Optimal Trajectories

The objective of this section of this report is to compare briefly various optimal entry missions from a standpoint of the guidance sensitivity requirements for effective trajectory control along the desired flight path. The discussion relates only to the principal control variable (roll angle) and no consideration is given to such factors as vehicle stabilization during the required maneuvers.

Consider entries of the type given in figure 4(a) for which maximum cross range was achieved with and without an altitude constraint imposed. The roll-angle histories for these entries include no rapid changes of a nature which would be difficult for an automatic or pilot-controlled system to follow. (Although roll angle is given in fig. 4(a) as a function of down range, the actual time histories followed a pattern similar to that shown.) However, it could be expected that unconstrained skip entries of this type would require more precise control than the altitude-limited cases because of the sensitivity of range to errors in the exit conditions. For example, on a skip trajectory such as that of figure 4(a) (h_x = 91.44 km, V_x = 6.9 km/sec, $\gamma_x = 1.05^o$), an error in ballistic range of 50 nautical miles occurs for each 0.1^o error in exit flight-path angle, as is shown in reference 12. Thus, although skip trajectories are advantageous from a heating standpoint (as previously shown), they may be more sensitive to control errors than altitude-limited entries.

The control-variable histories for minimum range entries also exhibit a slowly varying nature, as is shown in figure 6. The appearance of these trajectories is possibly

deceptive since previous studies have shown that minimum range entries are demanding from a control standpoint (refs. 7 and 8). This condition results from the difficulty in controlling acceleration to the desired value and the corresponding dependence of minimum range on acceleration. An additional complication for these trajectories is that the short entry times involved (3 minutes or less) allow little margin for error.

An examination of minimum heat trajectories given previously shows that the roll-angle variations are more rapid than was the case for minimum or maximum cross-range entries. However, these roll rates are still generally found to be of a reasonable nature. For example, the 180° change in roll angle shown in figure 8 occurred over a period of about 25 seconds. An analysis of the effect of altitude constraints on guidance sensitivities for minimum heat entries is similar to that already given for maximum cross-range entries.

SUMMARY OF RESULTS

The results of a study conducted to investigate optimal performance boundaries, from considerations of maneuver capability and entry heating, for an Apollo type vehicle under entry conditions encountered during lunar return can be summarized as follows:

1. Maximum cross range generally increases with reduced entry angle for ranges greater than about 2000 nautical miles, whereas the reverse is true for shorter ranges. The resultant heating for these entries increases as the initial entry angle is reduced.

2. Maximum cross-range capability and the resultant heating increase as initial velocity is increased.

3. Realistic constraints on skip altitude result in small decreases in maximum cross-range capability but lead to proportionately larger increases in the resultant heating.

4. In general, minimum convective heat trajectories are characterized by large acceleration pulses and ballistic skips, whereas maximum convective heat trajectories feature low-altitude low-acceleration flight paths.

5. The general effect of acceleration and altitude constraints on minimum and maximum heat boundaries is an increase in the minimum boundary as the acceleration level or skip altitude is lowered; thus, the spread of heating values attainable is reduced.

6. For a particular range condition, the level of the minimum and maximum heat boundaries increases almost linearly as initial entry angle is reduced and as initial velocity is increased. As the increase in the upper boundary is proportionally larger than for the lower one, the net effect is a widening of the spread of heating values attainable.

7. Although radiative effects accounted for as much as 25 percent of the total heat input for the conditions assumed in the analysis, the general nature of minimum and maximum heat trajectories was largely determined by convective effects.

8. For a particular down range condition, the minimum heating attainable is reasonably constant over much of the cross-range capability of the vehicle, the large increase in heat input occurring as the maximum cross-range condition is approached. Thus, trade-offs exist between maneuver capability and entry heating.

9. Optimal trajectories for which final cross range is constrained to zero employ near-constant roll rates or a combination of constant roll rate and bang-bang type of control to achieve the desired trajectory.

10. Although reductions in vehicle lift-drag ratio place heavy penalties on maximum maneuver capability, the effect on entry heating is generally a beneficial one. Thus, trade-offs may exist between lift-drag ratio, maneuver capability, and entry heating.

11. Reductions in the ballistic parameter of the vehicle are beneficial from the standpoint of both optimal maneuver capability and entry heating.

12. The rotation of the earth and atmosphere has little effect on maximum cross-range capability for equatorial entries to the east or west. However, the increased velocity of the vehicle with respect to the atmosphere for western entries results in higher levels of minimum and maximum heating as compared with eastern entries. For entries to the north or south, the rotation effect influences maximum maneuver capability but has no apparent effect on optimal heating.

Langley Research Center,
National Aeronautics and Space Administration,
Langley Station, Hampton, Va., November 14, 1966,
125-17-05-01-23.

REFERENCES

1. Bryson, Arthur E.; Denham, Walter F.; Carroll, Frank J.; and Mikami, Kinya.: Determination of Lift or Drag Programs To Minimize Re-Entry Heating. J. Aerospace Sci., vol. 29, no. 4, Apr. 1962, pp. 420-430.

2. Bryson, Arthur E., Jr.; Mikami, Kinya; and Battle, C. Tucker: Optimum Lateral Turns for a Re-Entry Glider. Aerospace Eng., vol. 21, no. 3, Mar. 1962, pp. 18-23.

3. Anon.: Three-Dimensional Trajectory Optimization Study. Space Inform. Systems Div., Raytheon Co., Sept. 25, 1964.
   Part I.- Blanton, H. Elmore: Optimum Programming Formulation. BR 3136-1 (Contract NAS1-4056).
   Part II.- Goodell, Ralph S.: Computer Program and User's Manual BR 3136-2 (Contract NAS1-4056).

4. Nerem, Robert M.; and Stickford, George H.: Shock Layer Radiation During Hypervelocity Re-Entry. AIAA Entry Technology Conference, CP-9, Am. Inst. Aeron. Astronaut., Oct. 1964, pp. 158-169.

5. Cosgriff, Robert Lien: Nonlinear Control Systems. McGraw-Hill Book Co., Inc., 1958.

6. Creer, Brent Y.; Smedal, Harald A.; and Wingrove, Rodney C.: Centrifuge Study of Pilot Tolerance to Acceleration and the Effects of Acceleration on Pilot Performance. NASA TN D-337, 1960.

7. Wingrove, Rodney C.: A Study of Guidance to Reference Trajectories for Lifting Reentry at Supercircular Velocity. NASA TR R-151, 1963.

8. Young, John W.; and Russell, Walter R.: Fixed-Base-Simulator Study of Piloted Entries Into the Earth's Atmosphere for a Capsule-Type Vehicle at Parabolic Velocity. NASA TN D-1479, 1962.

9. Grant, Frederick C.: Simple Formulas for Stagnation-Point Convective Heat Loads in Lunar Return. NASA TN D-890, 1961.

10. Kotanchik, J. N.; and Erb, R. B.: The Design of Thermal Protection Systems. Paper presented at 7th International Aeronautical Congress (Paris, France), June 14-16, 1965.

11. Lundell, John H.; Wakefield, Roy M.; and Jones, Jerold W.: Experimental Investigation of a Charring Ablative Material Exposed to Combined Convective and Radiative Heating in Oxidizing and Nonoxidizing Environments. AIAA Entry Technology Conference, CP-9, Am. Inst. Aeron. Astronaut., Oct. 1964, pp. 216-227.

12. Young, John W.: Study of the Use of Terminal Control Techniques for Guidance During Direct and Skip Entries for a Capsule-Type Vehicle at Parabolic Velocity. NASA TN D-2055, 1964.

NASA-Langley, 1967 —— 30 L-5218

"The aeronautical and space activities of the United States shall be conducted so as to contribute . . . to the expansion of human knowledge of phenomena in the atmosphere and space. The Administration shall provide for the widest practicable and appropriate dissemination of information concerning its activities and the results thereof."

—NATIONAL AERONAUTICS AND SPACE ACT OF 1958

NASA SCIENTIFIC AND TECHNICAL PUBLICATIONS

TECHNICAL REPORTS: Scientific and technical information considered important, complete, and a lasting contribution to existing knowledge.

TECHNICAL NOTES: Information less broad in scope but nevertheless of importance as a contribution to existing knowledge.

TECHNICAL MEMORANDUMS: Information receiving limited distribution because of preliminary data, security classification, or other reasons.

CONTRACTOR REPORTS: Scientific and technical information generated under a NASA contract or grant and considered an important contribution to existing knowledge.

TECHNICAL TRANSLATIONS: Information published in a foreign language considered to merit NASA distribution in English.

SPECIAL PUBLICATIONS: Information derived from or of value to NASA activities. Publications include conference proceedings, monographs, data compilations, handbooks, sourcebooks, and special bibliographies.

TECHNOLOGY UTILIZATION PUBLICATIONS: Information on technology used by NASA that may be of particular interest in commercial and other non-aerospace applications. Publications include Tech Briefs, Technology Utilization Reports and Notes, and Technology Surveys.

Details on the availability of these publications may be obtained from:

SCIENTIFIC AND TECHNICAL INFORMATION DIVISION

NATIONAL AERONAUTICS AND SPACE ADMINISTRATION

Washington, D.C. 20546